AD-A055 285 ARMY ELECTRONICS RESEARCH AND DEVELOPMENT COMMAND WS--ETC F/G 4/1
ABRES PRETEST ATMOSPHERIC MEASUREMENTS.(U)
APR 78 R O OLSEN, B W KENNEDY

UNCLASSIFIED ERADCOM/ASL-TR-0005 NL

| OF |
AD
A055285

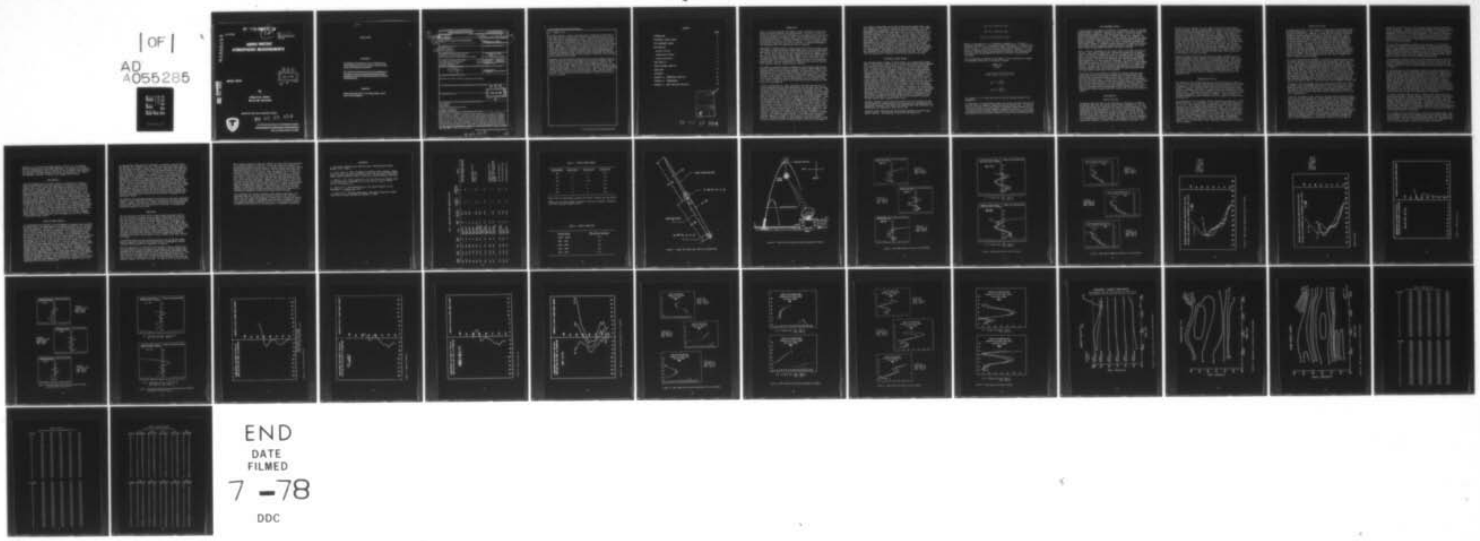

END
DATE
FILMED
7 -78
DDC

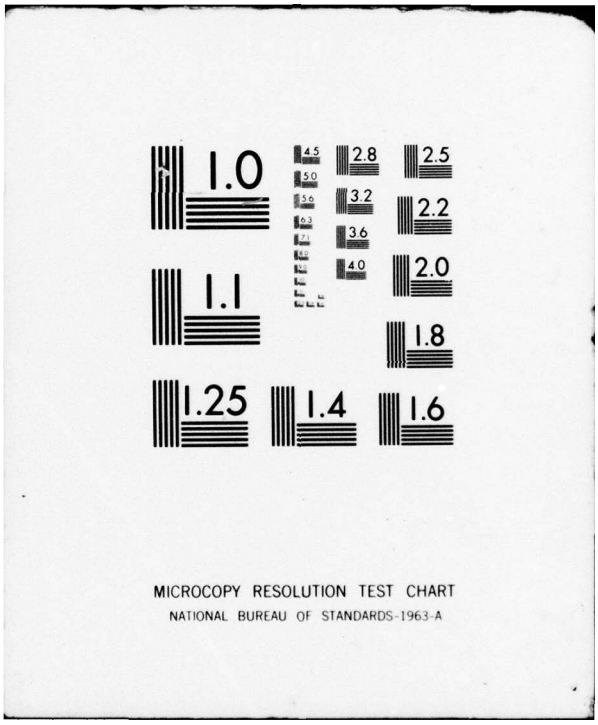

ASL-TR-0005

ABRES PRETEST ATMOSPHERIC MEASUREMENTS

APRIL 1978

By

Robert O. Olsen
Bruce W. Kennedy

Approved for public release; distribution unlimited.

US Army Electronics Research and Development Command
Atmospheric Sciences Laboratory
White Sands Missile Range, N.M. 88002

NOTICES

Disclaimers

The findings in this report are not to be construed as an official Department of the Army position, unless so designated by other authorized documents.

The citation of trade names and names of manufacturers in this report is not to be construed as official Government indorsement or approval of commercial products or services referenced herein.

Disposition

Destroy this report when it is no longer needed. Do not return it to the originator.

SECURITY CLASSIFICATION OF THIS PAGE (When Data Entered)

REPORT DOCUMENTATION PAGE

READ INSTRUCTIONS BEFORE COMPLETING FORM

1. REPORT NUMBER: ERADCOM/ASL-TR-0005
2. GOVT ACCESSION NO.:
3. RECIPIENT'S CATALOG NUMBER:
4. TITLE (and Subtitle): ABRES PRETEST ATMOSPHERIC MEASUREMENTS.
5. TYPE OF REPORT & PERIOD COVERED: Research and development R&D Technical Report
6. PERFORMING ORG. REPORT NUMBER:
7. AUTHOR(s): Robert O. Olsen, Bruce W. Kennedy
8. CONTRACT OR GRANT NUMBER(s):
9. PERFORMING ORGANIZATION NAME AND ADDRESS: Atmospheric Sciences Laboratory, White Sands Missile Range, New Mexico 88002
10. PROGRAM ELEMENT, PROJECT, TASK AREA & WORK UNIT NUMBERS: DA Task No. 1L162111AH71-B2
11. CONTROLLING OFFICE NAME AND ADDRESS: US Army Electronics Research and Development Command, Adelphi, MD 20783
12. REPORT DATE: April 1978
13. NUMBER OF PAGES: 47
14. MONITORING AGENCY NAME & ADDRESS (if different from Controlling Office): 45p.
15. SECURITY CLASS. (of this report): UNCLASSIFIED
15a. DECLASSIFICATION/DOWNGRADING SCHEDULE:

16. DISTRIBUTION STATEMENT (of this Report)

Approved for public release; distribution unlimited.

17. DISTRIBUTION STATEMENT (of the abstract entered in Block 20, if different from Report)

18. SUPPLEMENTARY NOTES

19. KEY WORDS (Continue on reverse side if necessary and identify by block number)

Stratosphere
Mesosphere
Robin inflatable falling sphere
Temporal variability
Spatial variability

20. ABSTRACT (Continue on reverse side if necessary and identify by block number)

Measurements of atmospheric parameters were obtained by utilizing inflatable falling sphere sensors. A series of these spheres were launched on 4 separate days. The first three series consisted of measurements from paired soundings and the last series consisted of four soundings made over a period of approximately 3 hours. The primary purpose of this study was to examine the spatial and temporal variations in atmospheric density between the altitudes of 60 and 90 km utilizing the operational inflatable falling sphere system and determine if this type of system would be capable of providing atmospheric data in support

DD FORM 1 JAN 73 1473 EDITION OF 1 NOV 65 IS OBSOLETE

SECURITY CLASSIFICATION OF THIS PAGE (When Data Entered)

20. ABSTRACT (cont)

of reentry missions. Results from these series of soundings indicate that in most cases density variations did not exceed 4%, within periods varying from less than an hour to approximately 3 hours. A portion of the density variation can be ascribed to instrumentation and system errors, which were calculated to be 2% over most of the altitude range. These results indicate that the atmospheric density variation in most cases was no more than 2% during these measurements. However, in the last series of launches, data were obtained which indicated large changes in atmospheric structure occurring at about 85 km. . These changes were observed in the density, temperature, and wind measurements and may be the result of an internal atmospheric gravity wave. By periodically sampling the atmosphere during the mission period, atmospheric cross sections can be constructed which permit a better estimate of the state of the atmosphere during the mission test periods.

Department of Defense agencies conducting ballistic missile reentry tests and studies at Kwajalein Missile Range (KMR) require accurate atmospheric measurements within the missile test environment from the surface to 100 km. The Air Force Space and Missile Systems Organization (SAMSO) sponsors most of the reentry programs at KMR. SAMSO is one of the prime drivers in generating upper atmospheric requirements for its particular tests. The Army's Ballistic Missiles Defense Command operates in two functional modes at KMR: they are responsible for operating the range and they perform defensive research against reentry vehicles. Therefore, results from this study are of interest to both the Air Force and the Army.

CONTENTS

INTRODUCTION

Vehicle tracking techniques and support systems involved in reentry missions have become elaborate and sophisticated. The result is that nonpredictive variations in the performance of the reentry vehicle may be due to some atmospheric perturbation rather than instrumentation error from ground-based sensors. It therefore becomes important to be able to separate atmospheric effects from vehicle effects. To fully evaluate these missions and reconstruct the reentry trajectory, a detailed knowledge of the atmosphere that the vehicles traverse is required.

Department of Defense agencies conducting ballistic missile reentry tests and studies at Kwajalein Missile Range (KMR) require accurate atmospheric measurements within the missile test environment from the surface to 100 km. The Air Force Space and Missile Systems Organization (SAMSO) sponsors most of the reentry programs at KMR. SAMSO is one of the prime drivers in generating upper atmospheric requirements for its particular tests. The Army's Ballistic Missiles Defense Command operates in two functional modes at KMR: they are responsible for operating the range and they perform defensive research against reentry vehicles.

An example of programs requiring atmospheric data exceeding the present sounding capabilities available at Kwajalein Missile Range (KMR) are the Advanced Ballistic Reentry System (ABRES), Thrusted Replica (TREP), Test Development Vehicle, and Maneuverable Reentry Vehicle programs. These programs require atmospheric density and wind measurements in the reentry corridor as the reentry vehicle moves through it. The TREP program requires upper atmospheric density measurements along the reentry trajectory from an altitude of 60 km to at least 100 km with accuracies in density to be less than ±5%.

To date, requirements for upper atmospheric data have been met by utilizing radiosonde balloons and meteorological rockets which have the capability of defining atmospheric structure from the surface to 70 km. The radiosonde is capable of measuring atmospheric parameters from the surface to 30 km and the rocketsonde from 20 to 70 km. Measurements at altitudes above 70 km require other types of systems such as rocket grenades, Pitot probe, rigid active sphere, and inflatable passive falling spheres. Each of these systems has its individual advantages and disadvantages. The two systems which were utilized in the ABRES pretest series are the rigid active sphere and the inflatable passive sphere, or Robin system. The rigid sphere is capable of obtaining atmospheric data over the altitude interval from 40 to 140 km and may be able to intersect a portion of the reentry corridor missions because of its greater range capability. However, this system is much larger and, more costly; consequently, it is limited in the number of soundings that can be made to support a reentry mission. The inflatable sphere system is relatively small and easily handled; therefore, a number of these units can be used to support a mission. Another advantage is that atmospheric wind data as well as densities are derived from the inflatable sphere, while the rigid sphere in

its present configuration can be used to derive only density data. Density, however, is of primary interest to Air Force programs. The inflatable spheres are dependent on precision radar track for derivation of atmospheric data, while the rigid sphere is not, since it contains an onboard accelerometer for obtaining data. The rigid sphere does utilize a precision radar track for altitude determination. However, a number of precision radars are located at this site and can be used for the inflatable sphere track. The disadvantage of the present Robin system is that measurements are restricted below an altitude of 90 km and the system does not have the range capability to intersect the reentry corridor. However, if the actual horizontal variability of density does not exceed 5%, then the inflatable sphere system can still provide the required density measurements. Consequently, an experiment with inflatable spheres was conducted to study the density variability over KMR. The results from this study are of interest to both the Air Force and the Army.

INFLATABLE SPHERE SYSTEM

The inflatable sphere system, or Robin sphere, is an operational system which is launched on a weekly basis from five Meteorological Rocket Network [1] stations to obtain data from 30 to 90 km. The Robin sphere system (Fig. 1) consists of the Super Loki booster motor and the Robin sphere dart. The dart achieves an apogee of 115 km after being drag separated from the booster motor. At apogee the folded sphere is deployed and is immediately inflated by residual air and the release of isopentane from a capsule contained within the sphere. The fully inflated sphere is 1 m in diameter and is constructed of metalized mylar which permits the sphere to be tracked by radars as it descends towards the surface (Fig. 2). To obtain high-quality density data, the spheres must be tracked by precision radars equivalent to an FPS-16 radar or better. At most of the ranges, the density data are derived by using one FPS-16 radar. The requirement for the precision radar track of the sphere is necessary for the accurate determination of velocities and accelerations, especially above 85 km where the small drag acceleration of the sphere makes accurate density measurements more difficult. With radars capable of greater accuracies and the utilization of coherently derived range-rate data, the atmospheric data above 85 km altitude can be improved; and it may be possible to derive accurate density data to approximately 95 km.

The Robin software utilizes the position data from the trajectory of the falling sphere to compute density, and then pressure is derived with the hydrostatic equation. Once density and pressure have been determined, the temperatures are computed by using the gas law.

The Robin sphere reduction uses the following equations to derive atmospheric density. The equations of motion of the sphere are:

$$m\ddot{x} = 1/2\ \rho\ Cd\ Av\ (\dot{x} - w_x)\ ,$$

$$m\ddot{y} = 1/2\ \rho\ Cd\ Av\ (\dot{y} - w_y)\ ,$$

$$m\ddot{z} = mg - 1/2\ \rho\ Cd\ Av\ (\dot{z} - w_z)\ ,$$

where m = mass sphere, x, y = horizontal coordinate, z = altitude, ρ = atmospheric density, Cd = drag coefficient of the sphere, A = sphere cross-sectional area, v = relative motion of sphere with respect to the air mass, and w = motion of the air mass relative to the earth. Dotted x, y, z coordinates indicate velocity and accelerations derived from radar position data and w with the designated subscript is the wind in the particular coordinate.

From the equations of motion of the sphere, a set of equations for computing atmospheric densities is derived as follows:

$$\rho = \frac{2m(\ddot{z} - g)}{Cd\ Av\dot{z}}\ ,$$

$$v = \sqrt{(\dot{x} - w_x)^2 + (\dot{y} - w_y)^2 + \dot{z}^2}\ ,$$

$$w_x = \dot{x} - \frac{\ddot{x}\ z}{\ddot{z} - g}\ ,$$

$$w_y = \dot{y} - \frac{\ddot{y}\ \dot{z}}{\ddot{z} - g}\ ,$$

and assume w = 0, or that there are no vertical motions present in the atmosphere.

An examination of these equations shows that precise position data derived from the radar are needed in computing accurate density data. A report by Luers [2] contains a full description of the Robin sphere program and the limitations associated with computing atmospheric densities. In its present operating mode, the Robin sphere system is capable of obtaining density measurements over the altitude interval of 60 km to near 90 km within ±5%.

THE EXPERIMENT DESIGN

To study spatial and temporal variability, simultaneous launch of two Robin sphere systems in opposite directions was initially planned to achieve the maximum spatial separation. Additional soundings, 1 to 2 hours later, would have determined the effects of temporal variability. However, because of the operational constraints, it was necessary to modify the experiment by launching in opposite directions with an unavoidable elapsed time between soundings. This resulted in at least a 30-minute difference between sphere launches. Although launches were made in opposite directions, with maximum spatial separation between soundings, there was also a temporal variation associated with each of the sets of firings.

Table 1 contains information on the launch times, directions, and mission success. Twelve Robin spheres were launched and tracked by the range radars (two MPS-36) on Kwajalein as well as the KREMS radars on Roi-Namur. Two of the soundings did not provide useful data because of a premature sphere collapse. The table also indicates the time and distance differences between each of the successive soundings. The sample size of the measurements available for analysis is limited; however, it is anticipated that data obtained from later launches can be used to verify these first results. The data used in this analysis were obtained by averaging the derived atmospheric data from each of the MPS-36 radars which were made available shortly after each of the missions.

In addition to an investigation of spatial and temporal density variations, data derived from the Robin program will be compared with data derived from a program developed by Xonics which utilizes radar range rate from the Alcor radar. A theoretical study by Xonics [3] determined that the inflatable sphere could be used to obtain data to 100 km altitude by utilizing range-rate data. This new program and the Robin program will be used, and the data from the two programs will be compared. This report is concerned only with atmospheric data obtained with the operational Robin sphere system; Xonics will analyze the various data reduction systems.

DATA ANALYSIS

Density Profiles

The density data from each of the soundings are presented in graphical and tabular form with the density values listed in Appendix A. The densities are plotted as a ratio with the 1966 US Standard Atmosphere. The utilization of the 1966 standard is an arbitrary choice which permits the density data to be presented on a linear scale with altitude, thereby resulting in a finer resolution display of the data. The density data from the first three series of launches are shown in Figs. 3a, b, and c. In Fig. 3a both of the profiles show a similarity in structure throughout the altitude interval of 65 to 90 km. There appears to be a relatively small-scale variation in density from one sounding to the other. The

second series of launches (Fig. 3b) shows a similarity in the density structure between the two soundings with the largest variation in the density ratios occurring between 85 and 89 km. Figure 3c is a plot of the density ratios from the soundings made on 21 August. Again there are similarities in structure between the paired soundings, with larger differences noted between each set of paired measurements. Of these three paired soundings the profiles obtained on 17 August (Fig. 3b) appear different from the other two sets at altitudes above 85 km. It was initially assumed that this may have been a diurnal feature since this set was launched 5 hours later than the other series. However, this assumption does not appear to be consistent because these measurements appear to be similar in structure to the first two launches on 31 August 1976 at 0112 UT and 0251 UT, indicating a random variation rather than one that can be attributed to a tidal variation.

Figure 4a shows basically the same results as those obtained from the earlier soundings. There appears to be an agreement in the overall vertical structure with some variation at different altitudes. The density ratios depicted in Fig. 4b are significantly different from the earlier paired soundings. There is a similarity in the density structure from 65 to 85 km; but in the altitude interval between 85 and 90 km, there is a relatively large variation in density from one sounding to the other with most of the variation restricted to altitudes above 85 km. This indicated a significant change in atmospheric structure which will be discussed later.

Temperature Profiles

The temperature data derived from the paired Robin spheres are shown in Figs. 5a, b, and c; and the tabulated data from these soundings are listed in Appendix B. These figures contain data derived from the first three series of launches. These data are plotted with the 1966 standard atmosphere as a reference for ease in viewing similarities between each of the paired series. The temperature profiles shown in Fig. 5a indicate similar structure and appear to be in general agreement. Figure 5b shows good agreement between the paired soundings, with the biggest differences occurring at 90 km.

An examination of Fig. 5c reveals similar temperatures between 65 to 78 km. Above 78 km there is a difference in temperature between the soundings of 10° to 12°C. This indicates that changes have occurred from sounding to sounding, with the changes taking place above 78 km. The first pair of soundings from the 31 August series (Fig. 6a) shows that the temperatures are generally in agreement except above 88 km. Figure 6b contains data from the second series of launches on 31 August, and there is little difference in the temperature profiles from 65 to 80 km. Above 80 km there is a large change in temperature. Again, the changes in atmospheric structure are occurring above 80 km, while below this altitude there appears to be, in most cases, little variation in temperature from sounding to sounding.

Density Variations

As pointed out earlier in this report, the operational constraints placed upon the program make it very difficult to determine density changes due to spatial variabililty. However, if there was little density variation between the paired soundings launched in different directions, and at different times, then there is evidence that both spatial and temporal variations are not a factor within the spatial and temporal confines of the paired observations. If there are changes in density between each successive launch, the change could be attributed to either temporal or spatial variation. Therefore, in the conduct of this investigation a finding of little or no change in density between successive launches, though not launched simultaneously, would indicate that spatial variation is not a factor and the density from the Robin sphere would be representative of a general area or location, since time can also be equated to a spatial variation. This assumption does not hold true if temporal and spatial effects cancel each other.

For a valid evaluation of atmospheric variability, the magnitude of errors in density that may influence the data must be examined. One of the factors to be considered is to what degree the data are affected by radar noise. This effect was determined by comparing the densities derived from the MPS-36A radar with the densities derived by the MPS-36B radar tracking the same sphere. Results of this analysis are shown in Fig. 7 where the error due to radar noise does not exceed 2%. The other error to consider is the bias error which is caused by the type of filter used in the Robin computer program. Luers calculated the magnitude of the bias error by simulation techniques [2]. The total error at various altitudes has been computed from data obtained from these series of soundings and the results are shown in Table 2. The total error varies between 2.0% and 3.6%.

The density variation between the paired soundings from the first series as shown in Fig. 8a indicates variations of less than 4% except at 70 km where the density ratio variation is 6.5%, and at 88 km where it is 5%. The density variation over the entire altitude range in this series is less than 4%, with time and horizontal spatial differences of 52 min and 94 km, respectively.

Figure 8b, the second series, shows two altitude intervals where the density ratio variation exceeds 4%. These intervals are at 86 to 87 km where the variation is 7% and at 66 to 67 km where it is 5.5%. Otherwise, the density ratio variation between the paired soundings does not exceed 4%. Figure 8c, the third series, indicates the density ratio variation does not exceed 4% with the exception of 5.5% at 82 to 83 km and 5% at 71 km. In the later case, there was a time variation only, since the spatial variation was less than 10 km at apogee. The density data from the soundings on 31 August are shown in Figs. 9a and b. Launches 2011 and 2012 show fairly typical variations as previously observed in the data from earlier paired measurements. The density ratio variation exceeds 4% only at 90 km; otherwise, the variations in density are less than 4%.

Figure 9b, the last series of this program, appears different from the earlier soundings. In this case the largest variations in density between any of the paired soundings is observed, indicating a large change in atmospheric structure in the upper atmosphere. The change in the density ratio at 65 km is 5.5%. It is less than 4% up to an altitude of 81 km, increasing to 6.2% at 83 km, then changing dramatically to a maximum in excess of 18% at 89 to 90 km. These values are the largest observed in any of the paired soundings.

The last pair of soundings indicates the occurrence of a disturbance resulting in relatively large-scale changes in density especially above 80 km. These changes are more apparent when the densities from the 2011 sphere launch at 0155 UT are compared to the last launch 2016 at 0512 UT. These two soundings indicate that the density structure had been altered rather rapidly in time, with the largest variation temporal since there was very little spatial variation between the soundings.

The rms density variation from 65 km to 90 km was computed for each pair of observations and the results are listed in Table 3. For each of the pairs of soundings, the rms density variation is less than 4% with the exception of the last pair of soundings where the rms variation in density is almost 7%.

As mentioned earlier, the operational constraints prevented the design of an experiment solely to determine spatial variability. However, it is possible to show a composite of time and space variability and determine whether the variability of both parameters is a factor. Figure 10 is a plot of the density ratio between all the paired soundings. The plot shows that the space and time variabilities are less than ±4% below 87 km, increasing to 8% between 87 and 90 km. Therefore, a conclusion may be drawn that in terms of both space and time there are variations in density but they are relatively small in scale and occur over small altitude intervals. The large variations at the upper end of the profile are attributed to the last two soundings, 2015 and 2016, where there appeared large changes due to some type of atmospheric disturbance.

The paired soundings made near 0200 UT (2001A, 2001B, 2008, 2009, 2011, and 2012) were used to analyze temporal variation in density to determine what type of density variations occurred over the less than 1-hour time period. Results of this analysis (Fig. 11) show very little variation between the first and second soundings. The maximum variation, 5%, occurs at 70 km, probably because of the Mach 1 transition in the sphere drag coefficients. Therefore, in undisturbed conditions there is no large-scale change in density over a time period of 1 hour or less during the time of day of these particular soundings.

In an attempt to more clearly define if there are any effects due to spatial variability, four of the launches were selected (2001A, 2001B, 2011 and 2012) where the first launch azimuth was made at 60° followed by the launch at 240°. The data from these soundings (Fig. 12) shows that there are no large differences in density due to space differences.

Figure 13 is a plot of the average density ratio for all 10 soundings with the extreme values from these soundings. The average is not useful for this investigation, but the range of values is because this represents the envelope of extreme density variations. As depicted in this figure the greatest variations in density occur between 85 and 90 km.

WIND PROFILES

The winds obtained from the several series of soundings are plotted in terms of wind direction and total magnitude as a function of altitude. Figures 14a, b, and c depict the wind direction measured from the first three series of launches. These plots show that the wind direction remains fairly consistent between each of the paired launches, but it can change considerably between each of the different launch series. Wind direction data from the series of launches on 31 August are shown in Figs. 15a and b. There appears the same consistency in the measured wind direction from each of the four series of soundings with the exception of the altitude interval between 85 to 90 km and from 65 to 70 km. The windspeed measurements obtained from the first three series of launches are plotted in Figs. 16a, b, and c; and again the same pattern is demonstrated as shown in the plots of the wind direction, indicating a consistency between each of the paired soundings and larger differences between each of the measurements made on different days. The launch series on 31 August reveal a large change in windspeed from 85 to 90 km (Figs. 17a, b) and a somewhat smaller change in wind magnitude occurring between 65 and 70 km, relative to the wind at other levels.

CROSS-SECTIONAL ANALYSIS

To investigate the variations in the thermodynamic parameters over a period of several hours, the measurements on 31 August were used to plot altitude-time cross sections. Figure 18 is a plot of the density ratio of the individual sounding to a mean density computation for altitude interval levels of 3 or 5 km as shown on the plotted figure. This representation shows how the densities changed at different levels in the atmosphere over the test period. This figure shows that the largest changes in density occurred at 90, 85, and 65 km. The cause of these variations is not known because the changes are in excess of the variations one could expect over this time period from strictly tidal effects. From this figure it can be shown that with sufficient measurements the state of the atmosphere can be readily defined within the confines of the measurement period. Related to the change in density there appear changes in temperature throughout the measurement period. These changes are shown in Fig. 19, a time-height cross section of the temperature field. The significant features in the temperatures are the cold temperatures occurring between 87 and 90 km as observed by the last sounding. This cooling coincides with a large increase in density at the same altitudes. Below the region of cooling, at 87 to 90 km, a warming interval occurs between 82 and 85 km which appears to be a compensating effect for the cooling above.

To complete the investigation of atmospheric variations, the wind field was plotted and is shown in Fig. 20. Here again the significant features are the large variations in winds above 85 km. Below this level there are some variations in the winds during the measurement period, but these are relatively small in comparison. In viewing the cross section of the density, temperature, and wind there appears to be a consistent pattern between each of the parameters. This is encouraging since densities and temperatures are related through the hydrostatic relationship. However, the winds are separate and independent from temperature and densities and the data reveal a corresponding variation at approximately the same altitudes. The occurrence of these features indicate the atmosphere can change rapidly over a relatively short period in the mesosphere. The sources of these changes remain a difficult problem to pinpoint directly, but the magnitude of the changes exceeds the normal diurnal tidal influences and the observed variations could be due to gravity waves which reached these levels at some other point and have been horizontally propagated to the measurement region.

The region of the atmosphere between 70 and 100 km is relatively unexplored compared to the region below 70 km where rocketsondes have been used extensively. However, there have been studies by Theon and Faire [4,5] which indicate that there can be large short-term variations in thermodynamic parameters between 90 and 100 km.

CONCLUSION

The data obtained from these series of Robin sphere soundings indicate that the variation in density due to temporal differences of an hour or less and spatial differences of 100 km does exceed an rms value of ±4%, with the exception of shallow altitude intervals (1 to 2 km) where the variation can be as large as 6% to 7%. These figures are slightly above the calculated system errors which vary from 4.2% at 90 km to 2% at 65 km. Though there appears to be no large-scale variation in most of these soundings, the last soundings (2015 and 2016 on 31 August) indicate a large variation of density above 85 km. These rapid changes in atmospheric structure above 85 km are indicative of gravity waves which can alter atmospheric structure and are known to occur randomly since their sources are varied.

The possible sources of gravity waves are many, such as the jet stream, aurora, orographic features, and instabilities at tropospheric heights. Therefore their occurrence is impossible to predict.

With the possibility of relatively large changes in density above 85 km, the requirement for accurate density in the reentry corridor becomes more dependent on the temporal variation rather than spatial variations since the velocity of the gravity wave can be greater than 900 km per hour. This would lead one to propose that the density measurements be made in the order of tens of minutes prior or after the reentry mission, and have the sounding traverse the reentry corridor. In lieu of this, one could launch

Robin spheres before and after each mission to insure that there have been no large-scale changes in density. In the event there are changes, the density measurements could be scaled to closely estimate the actual density measurement during the reentry mission. The conclusions drawn from this study are tentative at this point. Since the sample size is limited and the data utilized in this study were from the MPS-36 radars, it would be very useful to perform a similar type analysis, utilizing data from the Alcor radar, a more precise radar, and the new range-rate program, which has a finer vertical resolution. However, with the addition of more data from the various mission support rounds, the results found in this investigation are expected to be verified, especially in regard to measurements above 80 km where there appears to be evidence at times of large-scale changes in atmospheric structure. Data from support missions and data obtained from projected routine soundings can be used as a data base for determining atmospheric variability at these higher altitudes.

The requirement for precise atmospheric data becomes urgent when it is understood that due to large cost involved in each of the individual tests, the tests cannot be repeated to statistically evaluate the various error sources. Rather, measurements have been made to completely define the reentry performance, reducing the error in the ground-based sensors and defining the error due to the uncertainty in atmospheric conditions.

REFERENCES

1. RCC Council Meteorological Working Group - Meteorological Rocket Network 111-42 (1964).

2. Luers, James K., 1970, "A Method of Computing Winds, Density, Temperature, Pressure, and Their Associated Errors from the High Altitude Robin Sphere Using an Optimum Filter," University of Dayton Research Institute.

3. Martin, L. R., and T. Azzarelli, 1976, "Utilization of Coherent Radar for Determination of Atmospheric Winds and Density," Xonics TR-001, Xonics, Los Angeles, CA.

4. Theon et al., "Some Observations on the Thermal Behavior of the Mesosphere," J. Atmos. Sci. 1967.

5. Faire et al., "Anomalous Mesospheric Temperatures Observed at White Sands Missile Range, New Mexico," COSPAR XII, 1969.

TABLE 1. ABRES DENSITY MEASUREMENT PROGRAM ROBIN SPHERES

Launch Number	Date (1976)	Time (UT)	Launch AZ(°)	Radars	Apogee (km)	Data (km) Top/Bottom	Δ Time Before Launch (Min)	Δ Distance Before Launch (km)	Remarks
2001A	28 Jul	0144	60	MPS-36(A&B) Alcor	114	90/31	--	--	MPS-36 with computer aided track (CAT) unless otherwise specified
2001B	28 Jul	0236	240	MPS-36(A&B) Alcor	115	90/29	52	94	
2003	17 Aug	0646	60	MPS-36(A&B) Alcor	115	90/32	--	--	
2004	17 Aug	0720	60	MPS-36(A&B) Alcor	116	--	--	--	Premature sphere collapse Data not valid
2005	17 Aug	0750	240	MPS-36(A&B) Alcor, Altair	106	90/34	64	110	Twilight launch
2008	21 Aug	0151	240	MPS-36(A&B) Alcor, Altair Tradex	113	90/32	--	--	
2009	21 Aug	0233	240	MPS-36(A&B) Alcor, Altair Tradex	115	90/33	43	<10	
2010	21 Aug	0303	240	MPS-36(A&B) Alcor	116	--	--	--	Premature sphere collapse Data not valid
2011	31 Aug	0155	60	MPS-36(A&B) Alcor, Tradex	115	90/30	--	--	MPS-36A non-cattrack, MPS-36B cattrack, servo bandwidth 3 on MPS-36A
2012	31 Aug	0251	240	MPS-36(A&B) Alcor, Tradex	115	90/30	99	109	MPS-36A servo bandwidth 3
2015	31 Aug	0402	240	MPS-36B Alcor	115	90/30	--	--	MPS-36A tracking met rocket
2016	31 Aug	0512	60	MPS-36(A&B) Alcor	115	90/30	70	115	MPS-36A bandwidth setting 4

TABLE 2. PERCENT RADAR ERRORS

Altitude(km)	Noise Error*	Bias Error**	Total Error
90	2	4	4.2
85	2	3	3.6
80	2	-1.5	2.5
75	2	-1	2.2
70	2	-1	2.2
<70	2	0	2.0

*Noise error is empirically computed from radars tracking the same sphere.

**Bias error is theoretically computed by utilizing simulation techniques with Robin computer programs (Ref 1).

TABLE 3. DENSITY VARIATION

Paired Series	RMS Density Variation
2001A - 2001B	3.2
2003 - 2005	3.5
2008 - 2009	3.3
2011 - 2012	2.6
2015 - 2016	6.9

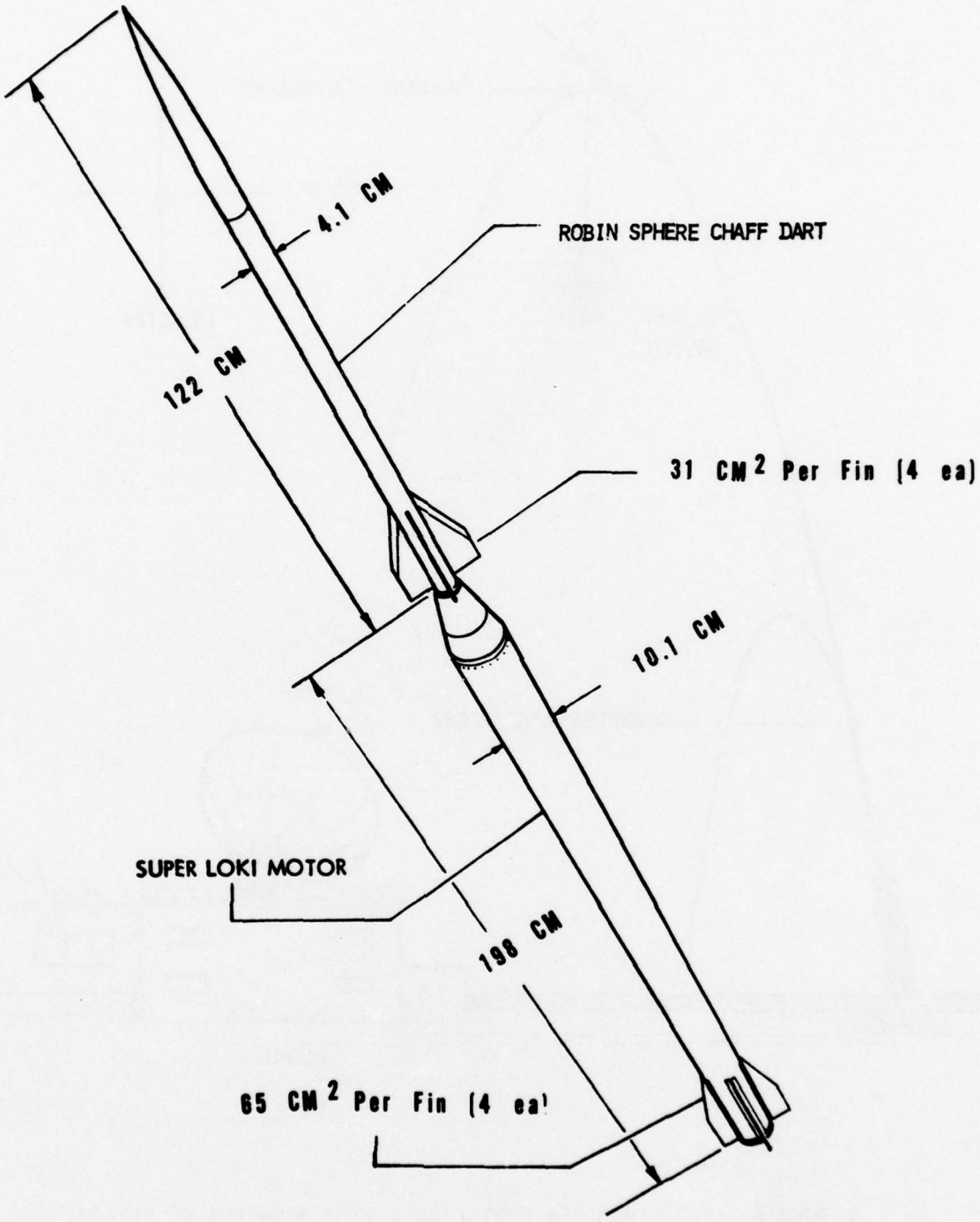

Figure 1. Super Loki Robin dart vehicle configuration.

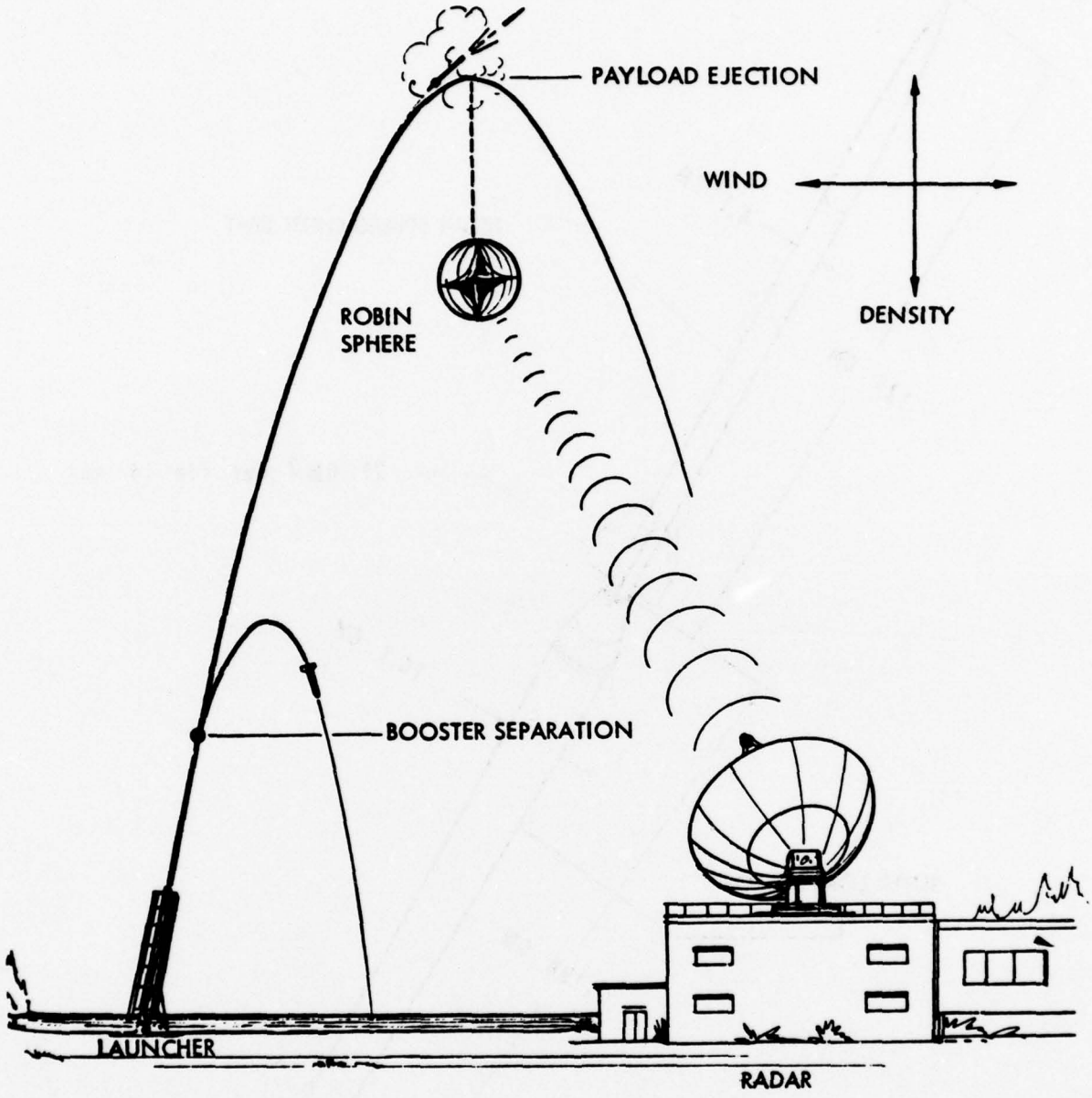

Figure 2. Robin density measuring system sequence of events.

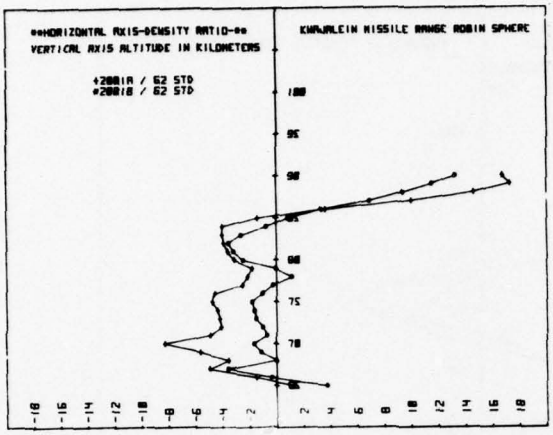

Figure 3a
28 July 1976
2001A - 0144 UT
2001B - 0236 UT

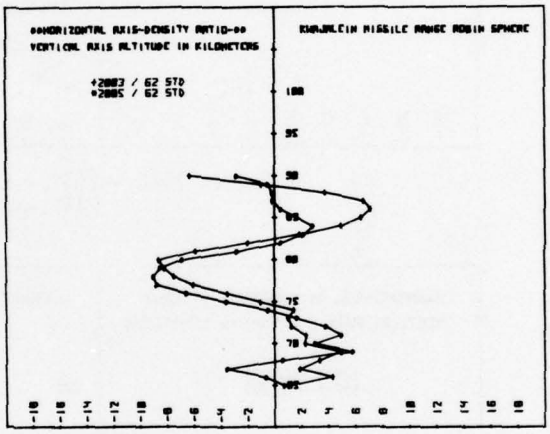

Figure 3b
17 August 1976
2003 - 0646 UT
2005 - 0705 UT

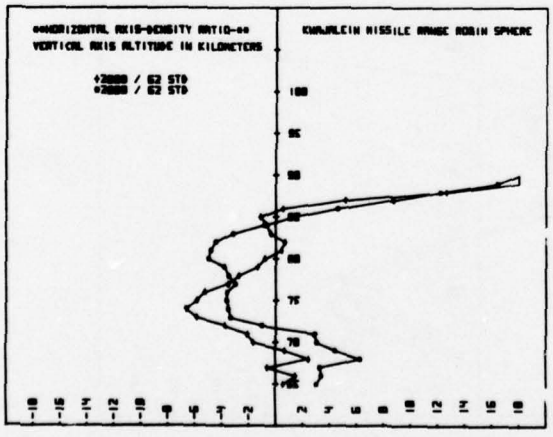

Figure 3c
21 August 1976
2008 - 0151 UT
2009 - 0233 UT

Figure 3. Robin sphere density ratios for July and August.

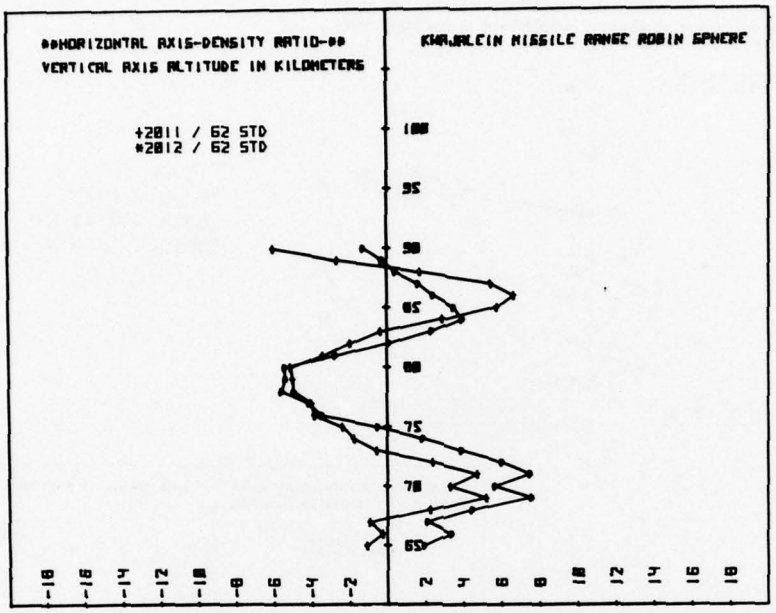

4a. 31 August 1976 - 2011 - 0112 UT
2112 - 0251 UT

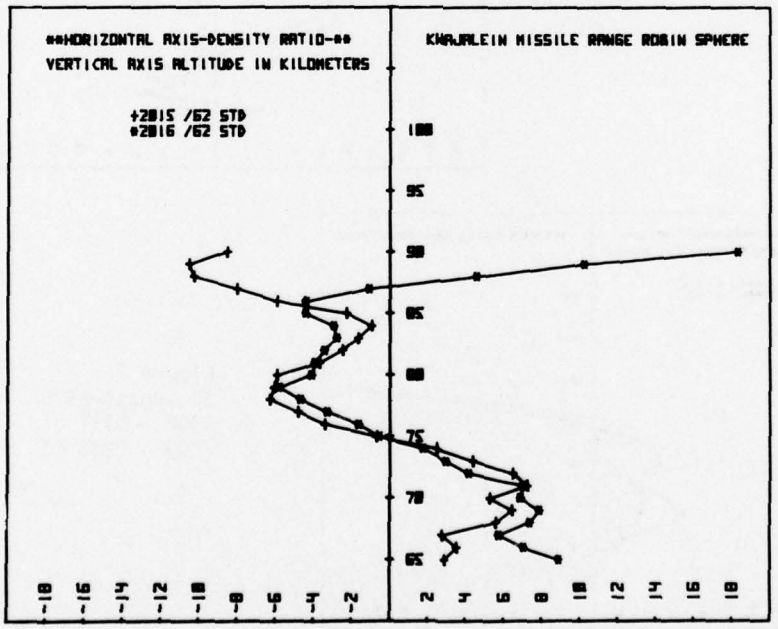

4b. 31 August 1976 - 2015 - 0402 UT
2016 - 0512 UT

Figure 4. Robin sphere density ratios for August.

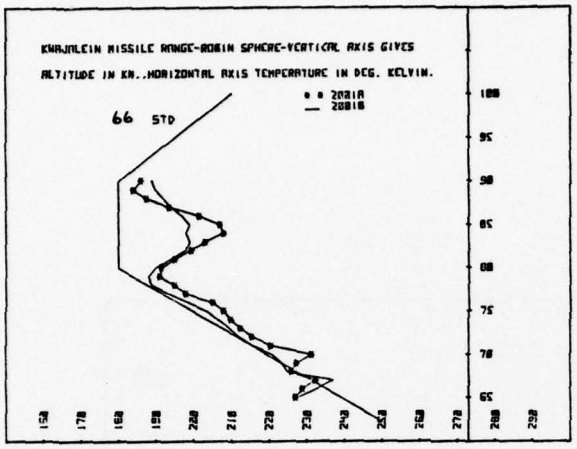

Figure 5a
28 July 1976
2001A - 0144 UT
2001B - 0236 UT

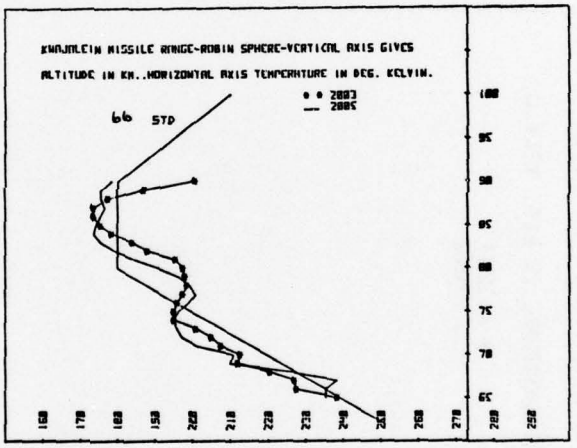

Figure 5b
17 August 1976
2003 - 0646 UT
2005 - 0750 UT

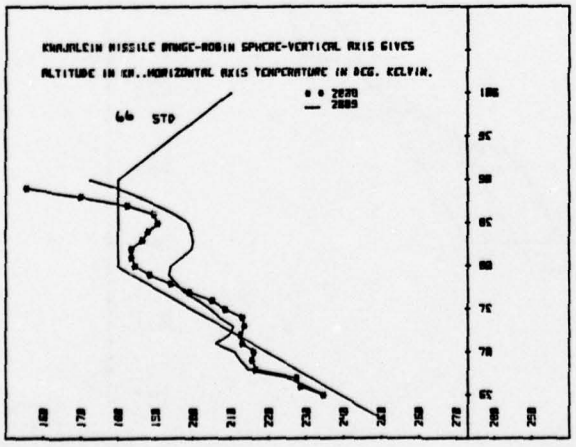

Figure 5c
21 August 1976
2008 - 0151 UT
2009 - 0233 UT

Figure 5. Robin sphere temperature profiles for July and August.

ing to sounding.

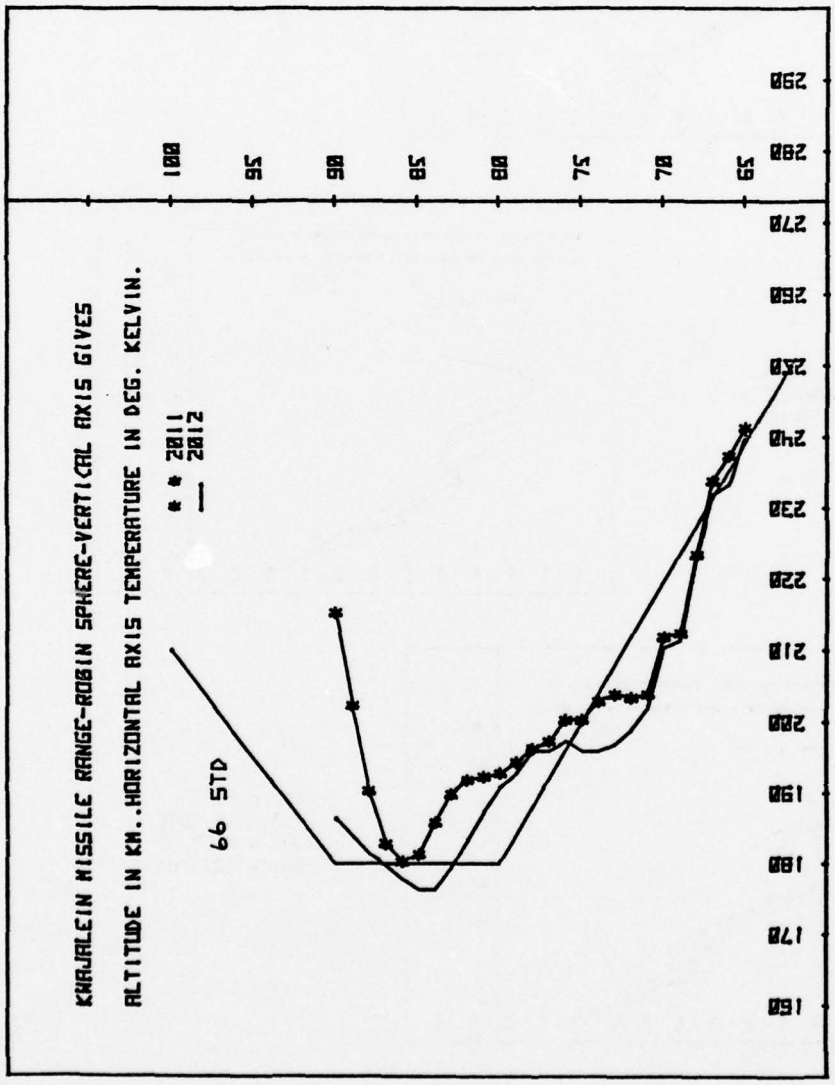

Figure 6a
31 August 1976
2011 - 0112 UT
2012 - 0251 UT

Figure 6. Robin sphere temperature profiles for August.

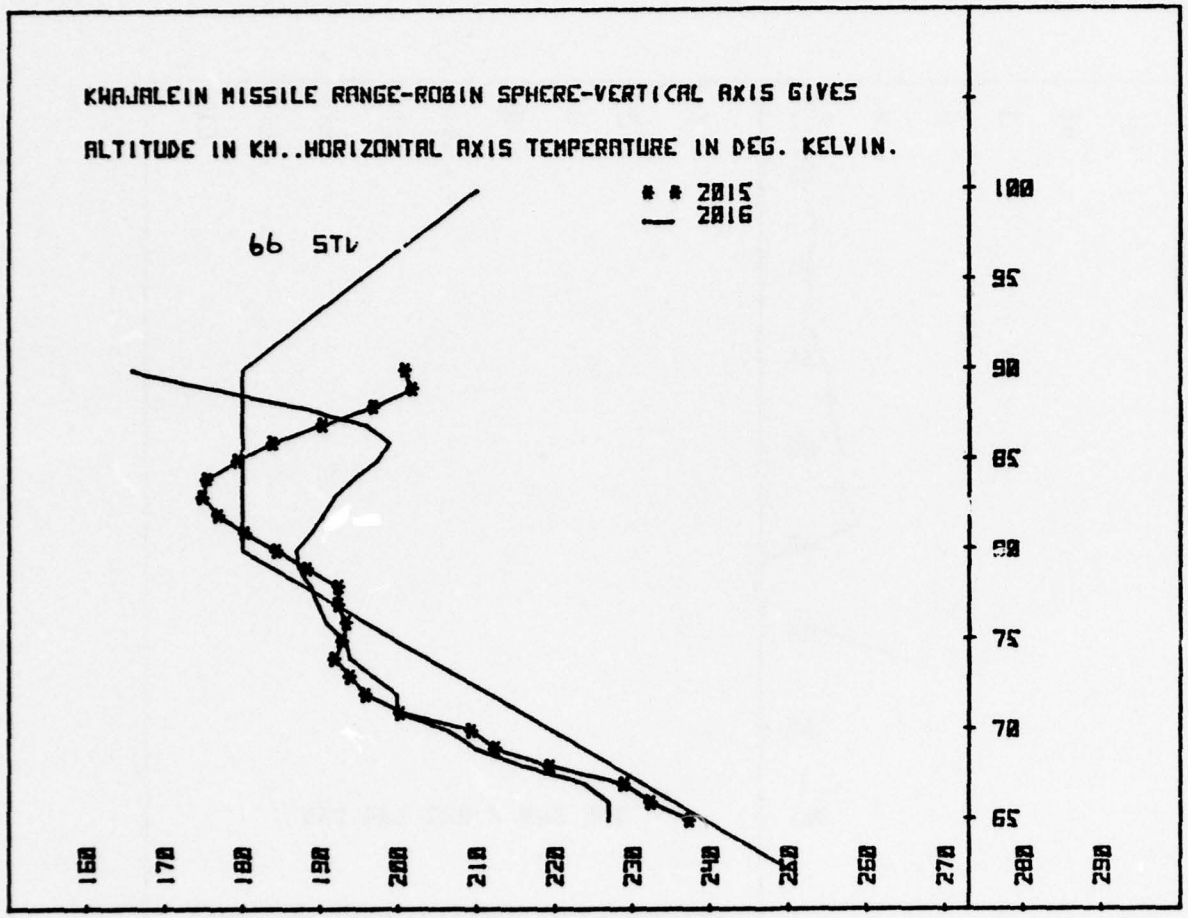

Figure 6b
31 August 1976
2015 - 0402 UT
2016 - 0512 UT

Figure 6 (cont)

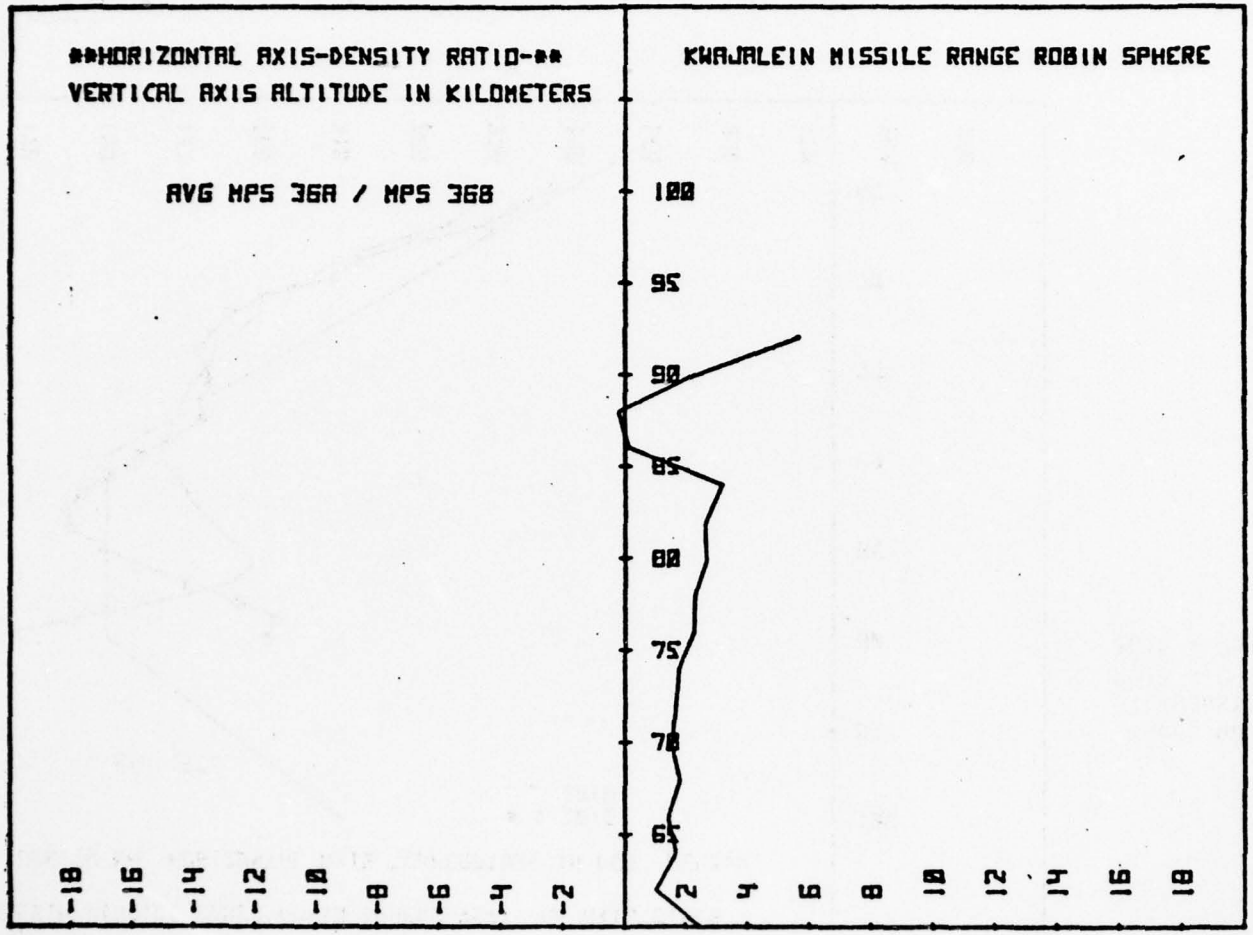

Figure 7. Radar noise error.

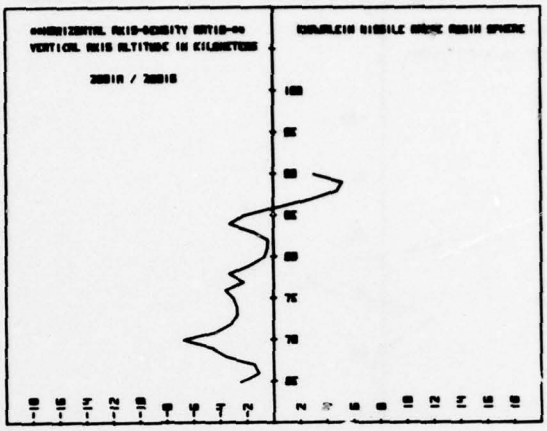

Figure 8a
Δ Distance = 94 km
Δ Time = 52 min
2001A - 0144 UT
2001B - 0236 UT

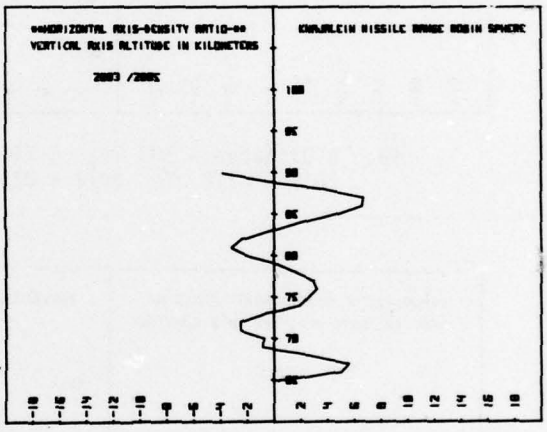

Figure 8b
Δ Distance = 110 km
Δ Time = 66 min
2003 - 0646 UT
2005 - 0750 UT

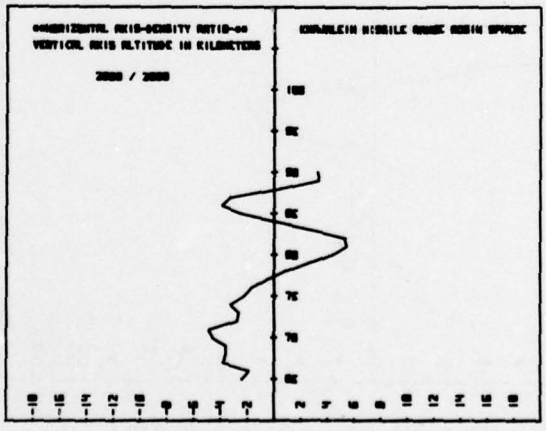

Figure 8c
Δ Distance = <10 km
Δ Time = 42 min
2008 - 0151 UT
2009 - 0233 UT

Figure 8. Robin sphere density ratios indicating spatial and temporal variability for 94, 110, and <10 km.

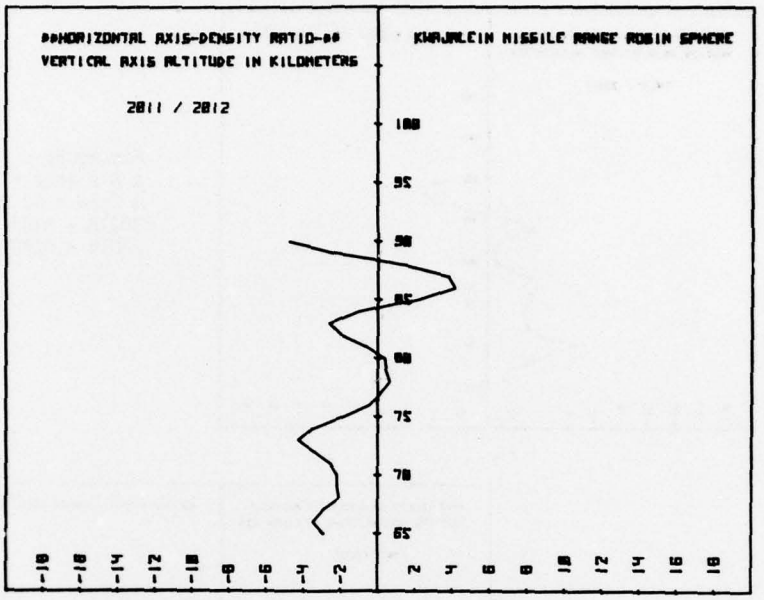

9a. Δ Distance = 109 km, Δ Time = 99 min
2011 - 0112 UT, 2012 - 0251 UT

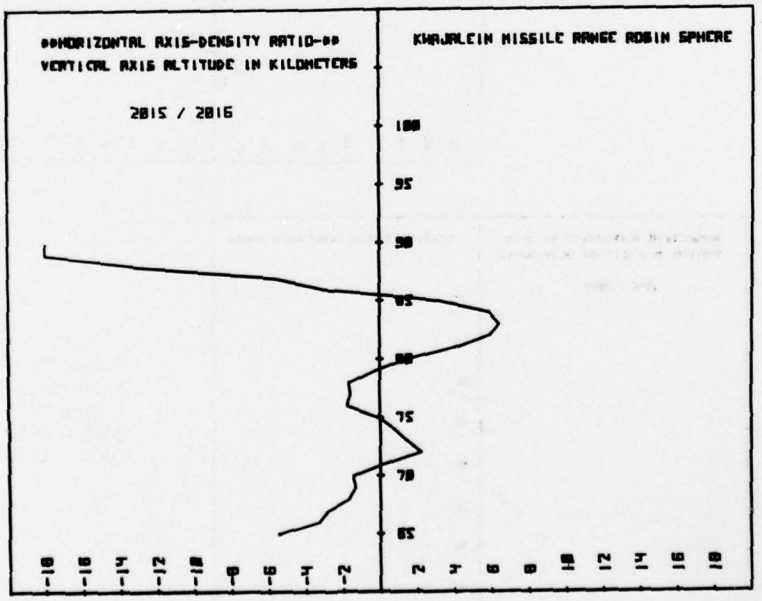

9b. Δ Distance = 115 km, Δ Time = 70 min
2015 - 0402 UT, 2016 - 0512 UT

Figure 9. Robin sphere density ratios indicating spatial and temporal variability for 109 and 115 km.

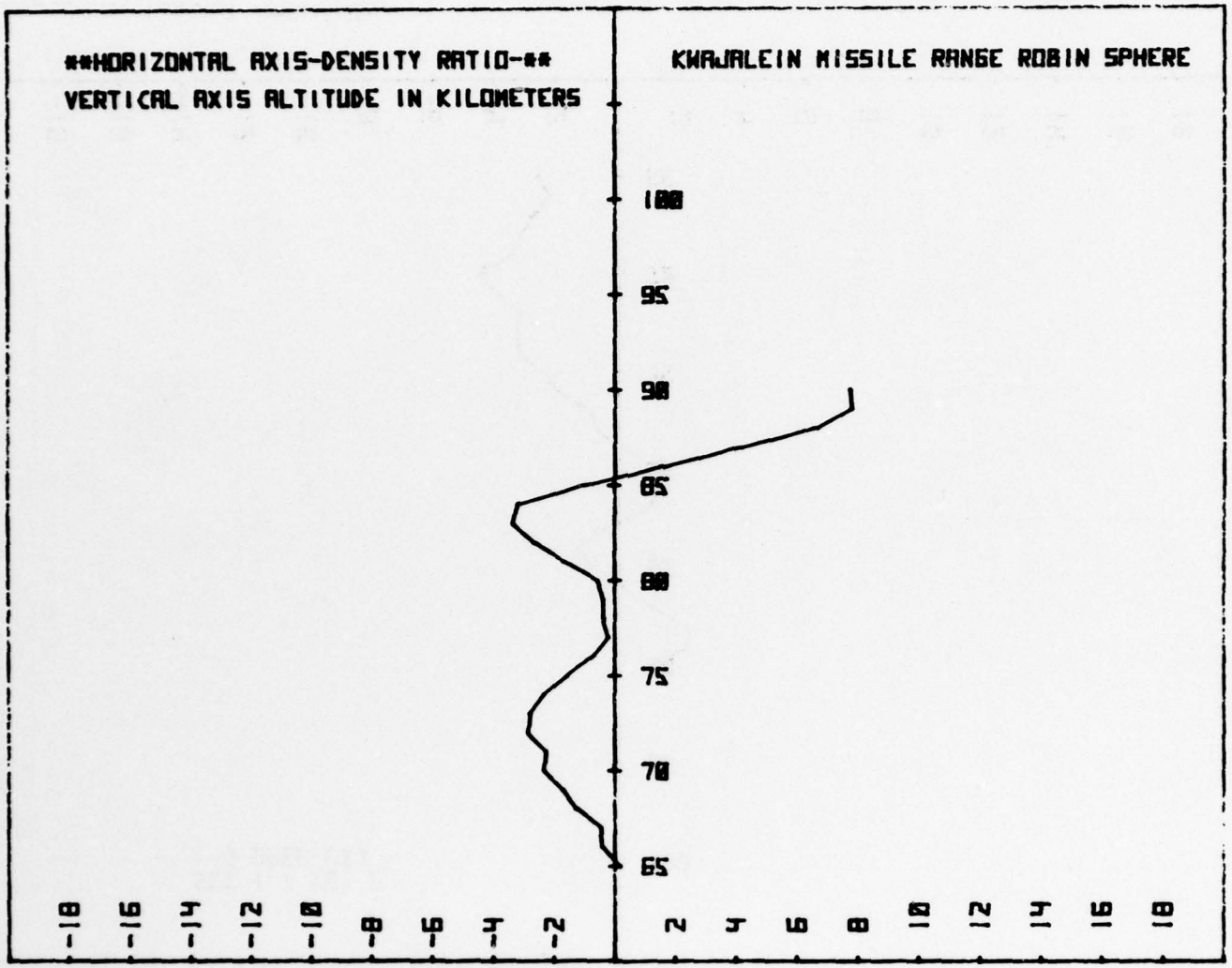

Three launches at 60° azimuth,
Five launches at 240° azimuth,
Time in all cases greater than 30 min.

Figure 10. Time and space variability.

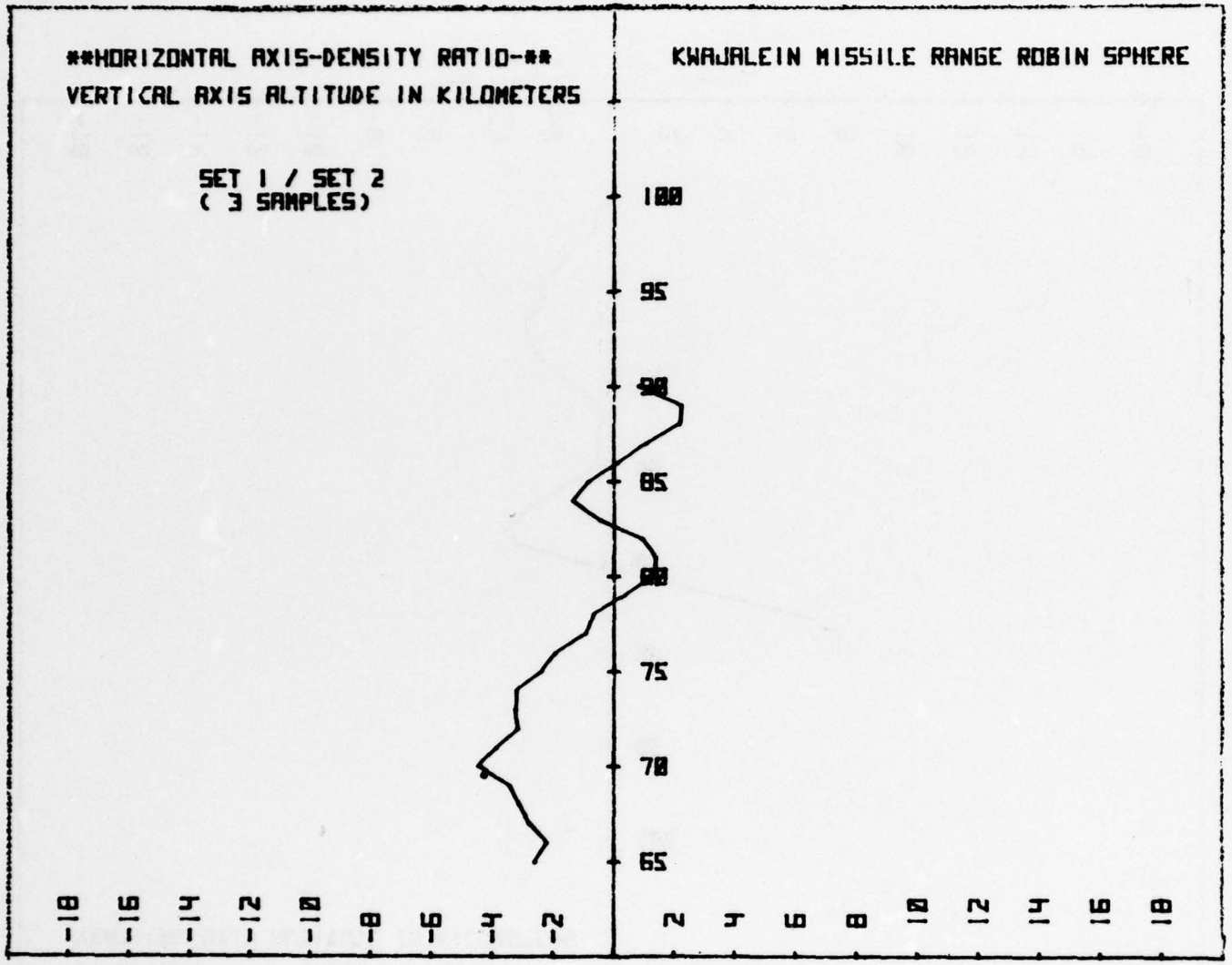

Figure 11. Temporal variability.

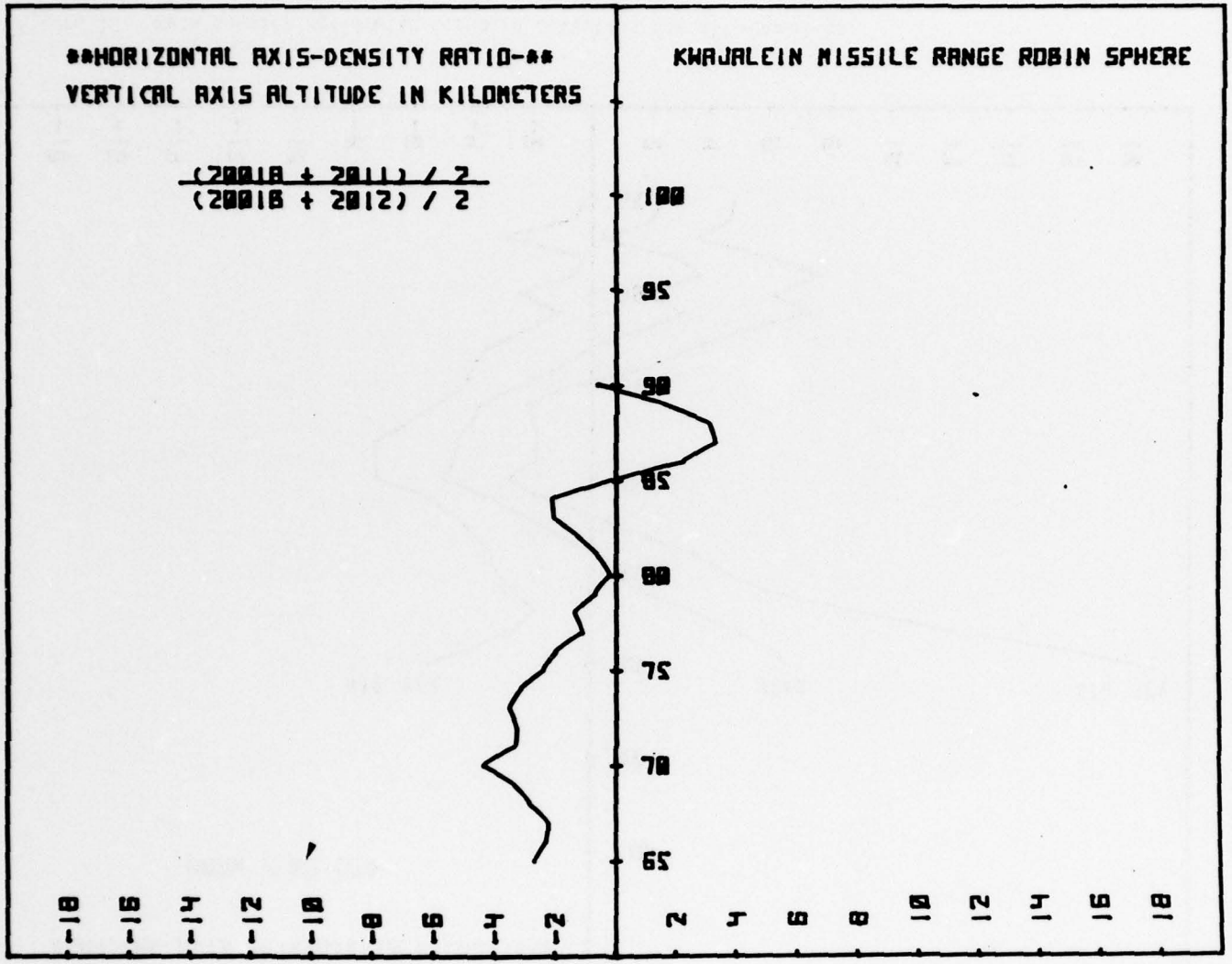

Figure 12. Spatial variability.

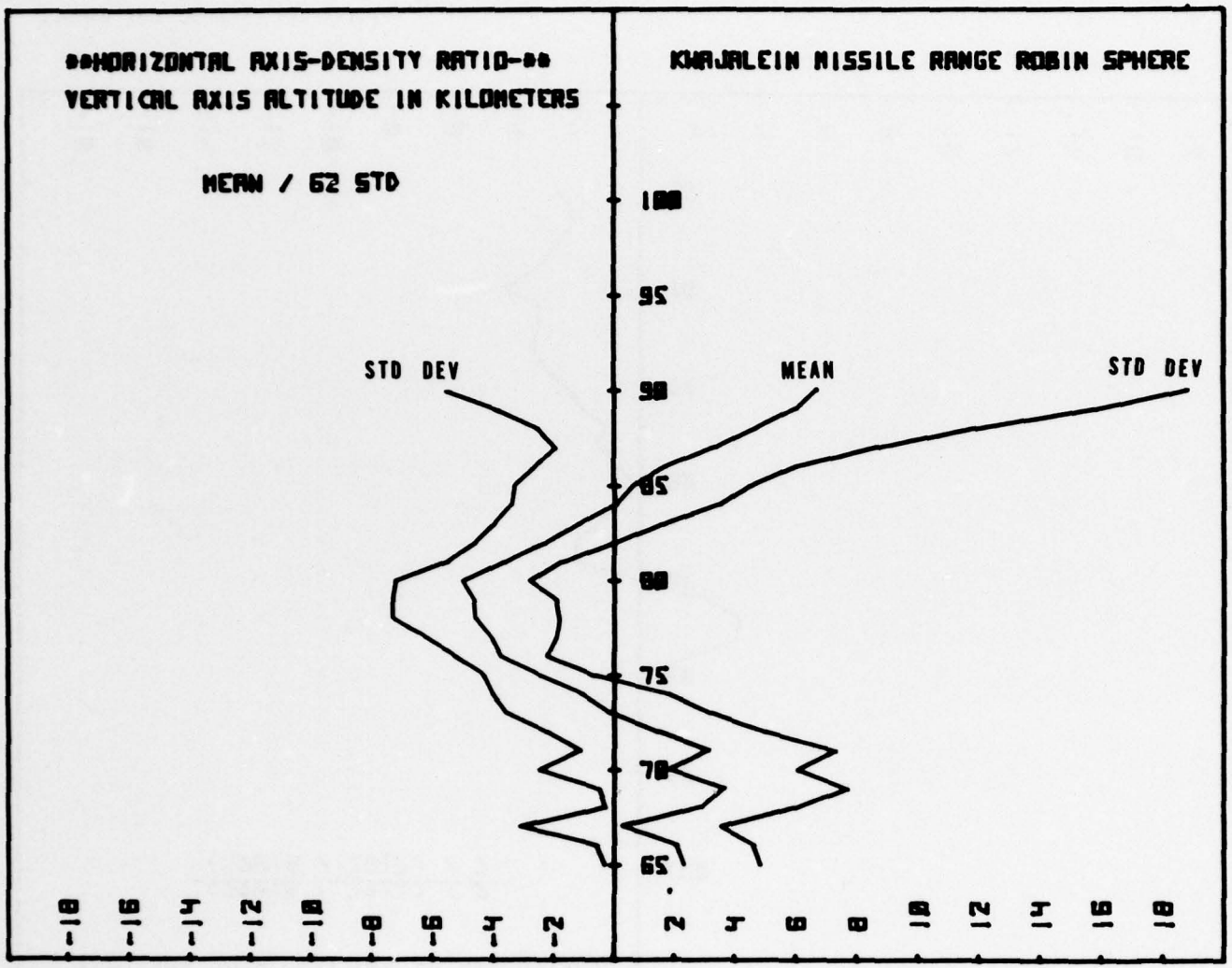

Figure 13. Mean density ratio with standard deviation for all soundings.

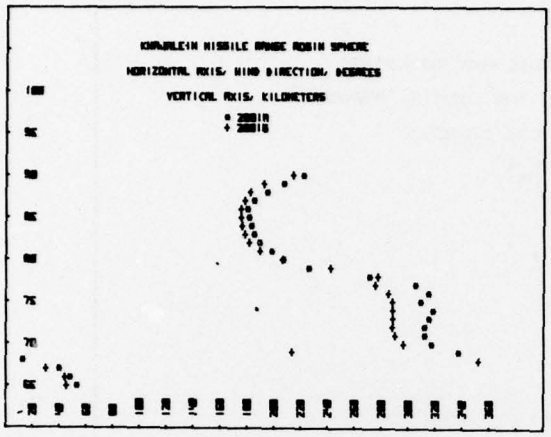

Figure 14a
28 July 1976
2001A - 0144 UT
2001B - 0236 UT

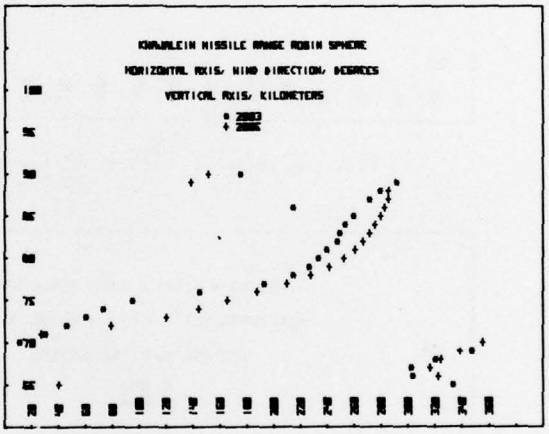

Figure 14b
17 August 1976
2003 - 0646 UT
2005 - 0750 UT

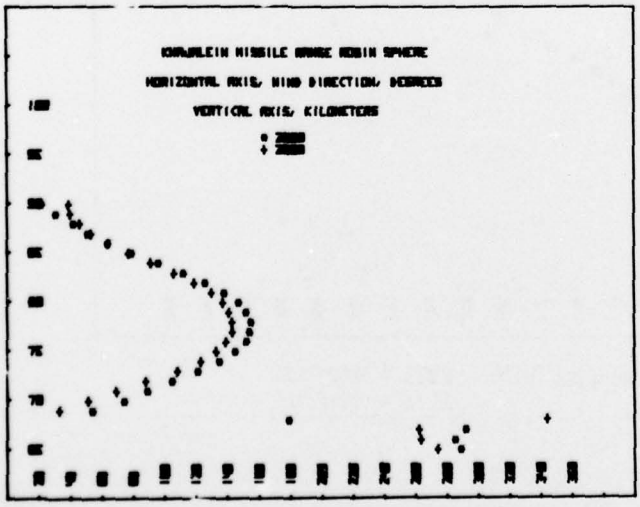

Figure 14c
21 August 1976
2008 - 0151 UT
2009 - 0233 UT

Figure 14. Robin sphere wind direction measurements for July and August.

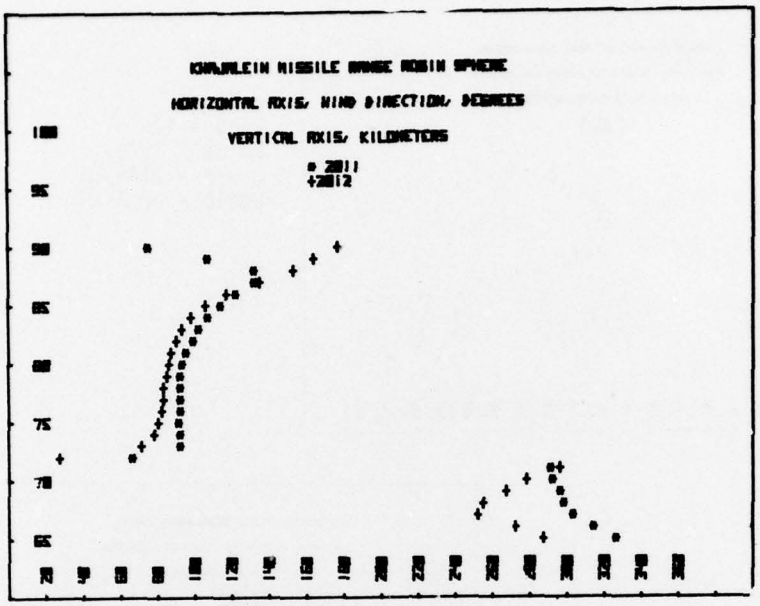

15a. 31 August 1976 - 2011 - 0112 UT
2012 - 0251 UT

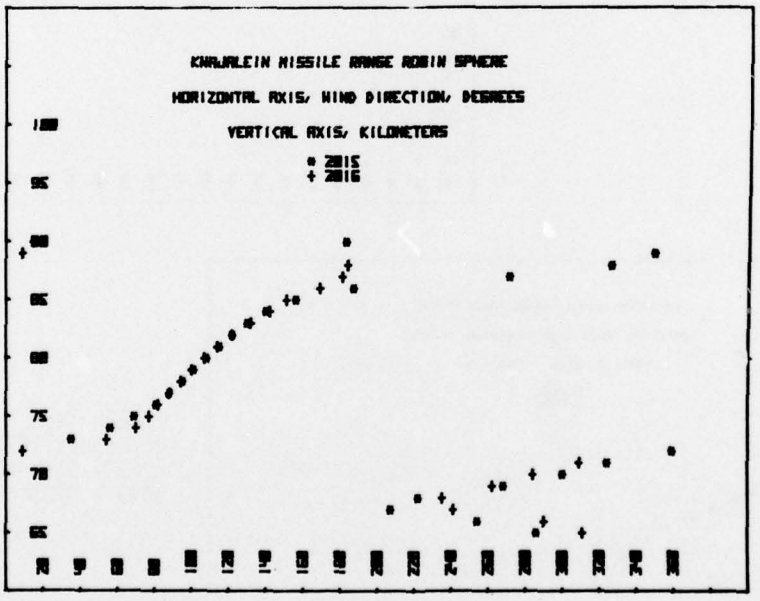

15b. 31 August 1976 - 2015 - 0402 UT
2016 - 0512 UT

Figure 15. Robin sphere wind direction measurements for August.

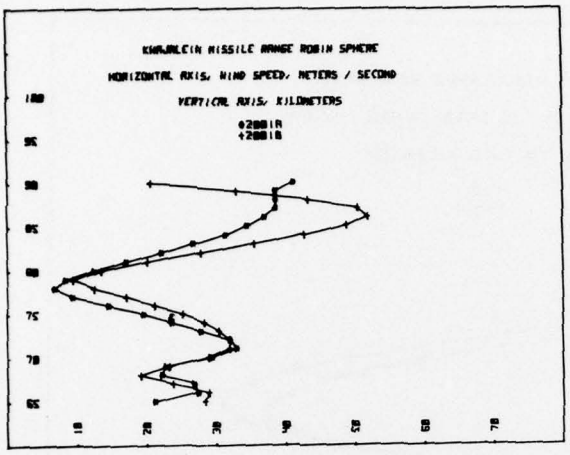

Figure 16a
28 July 1976
2001A - 0144 UT
2001B - 0236 UT

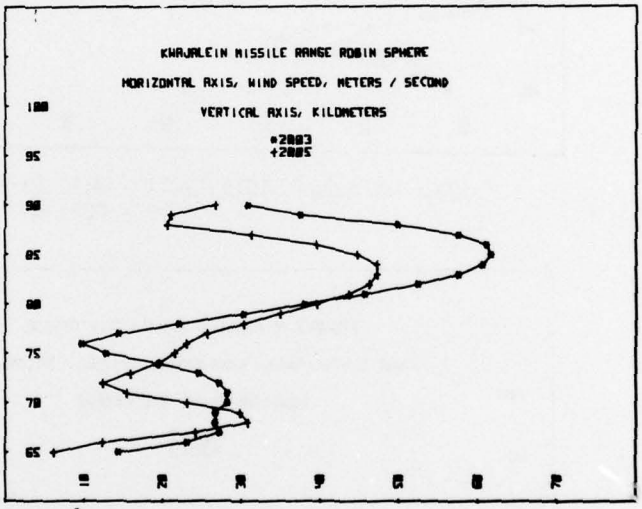

Figure 16b
17 August 1976
2003 - 0646 UT
2005 - 0750 UT

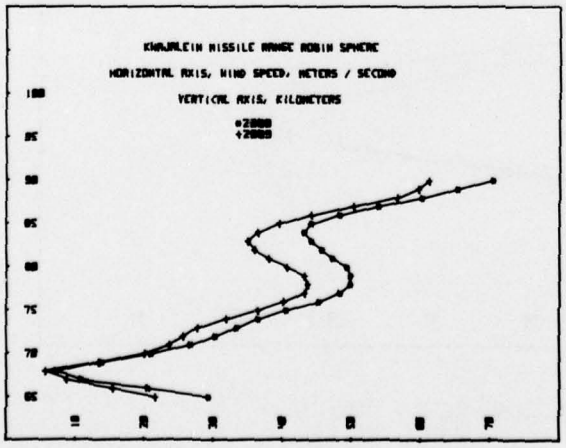

Figure 16c
21 August 1976
2008 - 0151 UT
2009 - 0233 UT

Figure 16. Robin sphere wind speed for July and August.

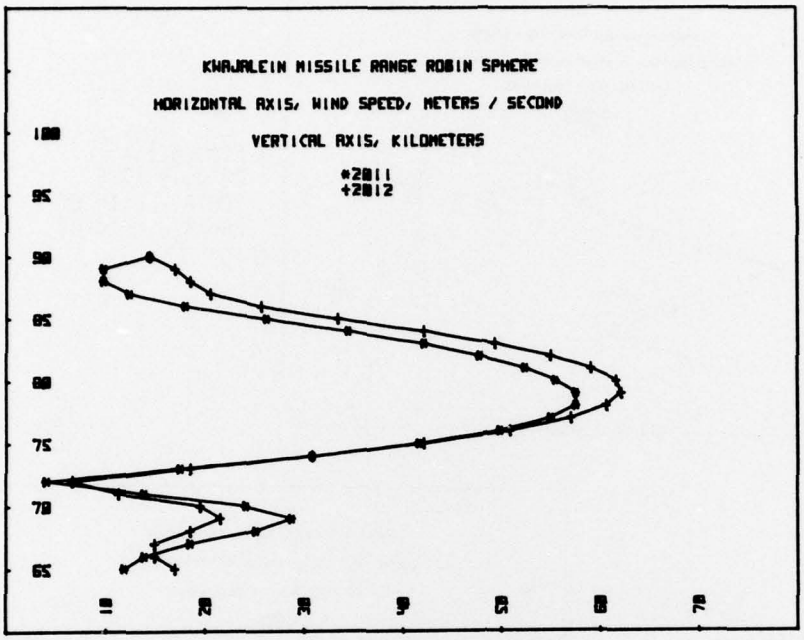

17a. 31 August 1976 - 2011 - 0112 UT
2012 - 0251 UT

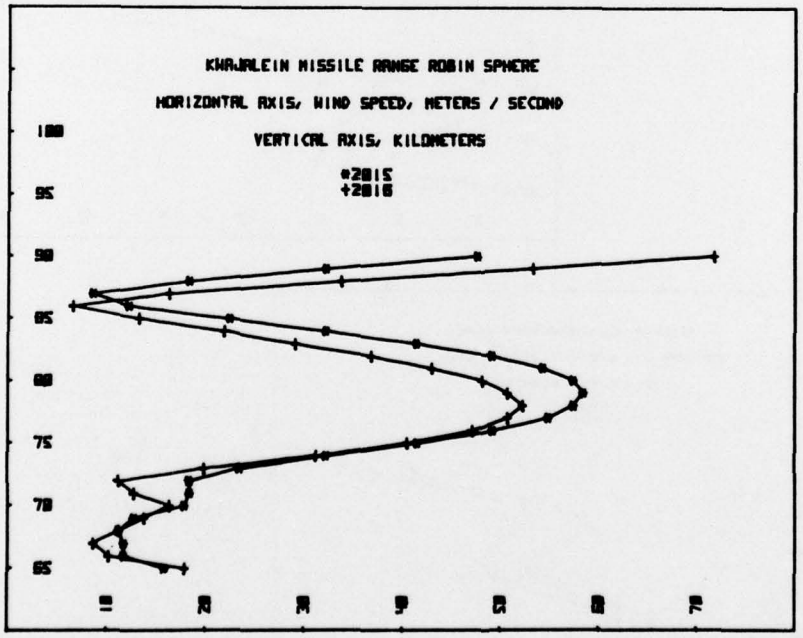

17b. 31 August 1976 - 2015 - 0402 UT
2016 - 0512 UT

Figure 17. Robin sphere wind speed for August.

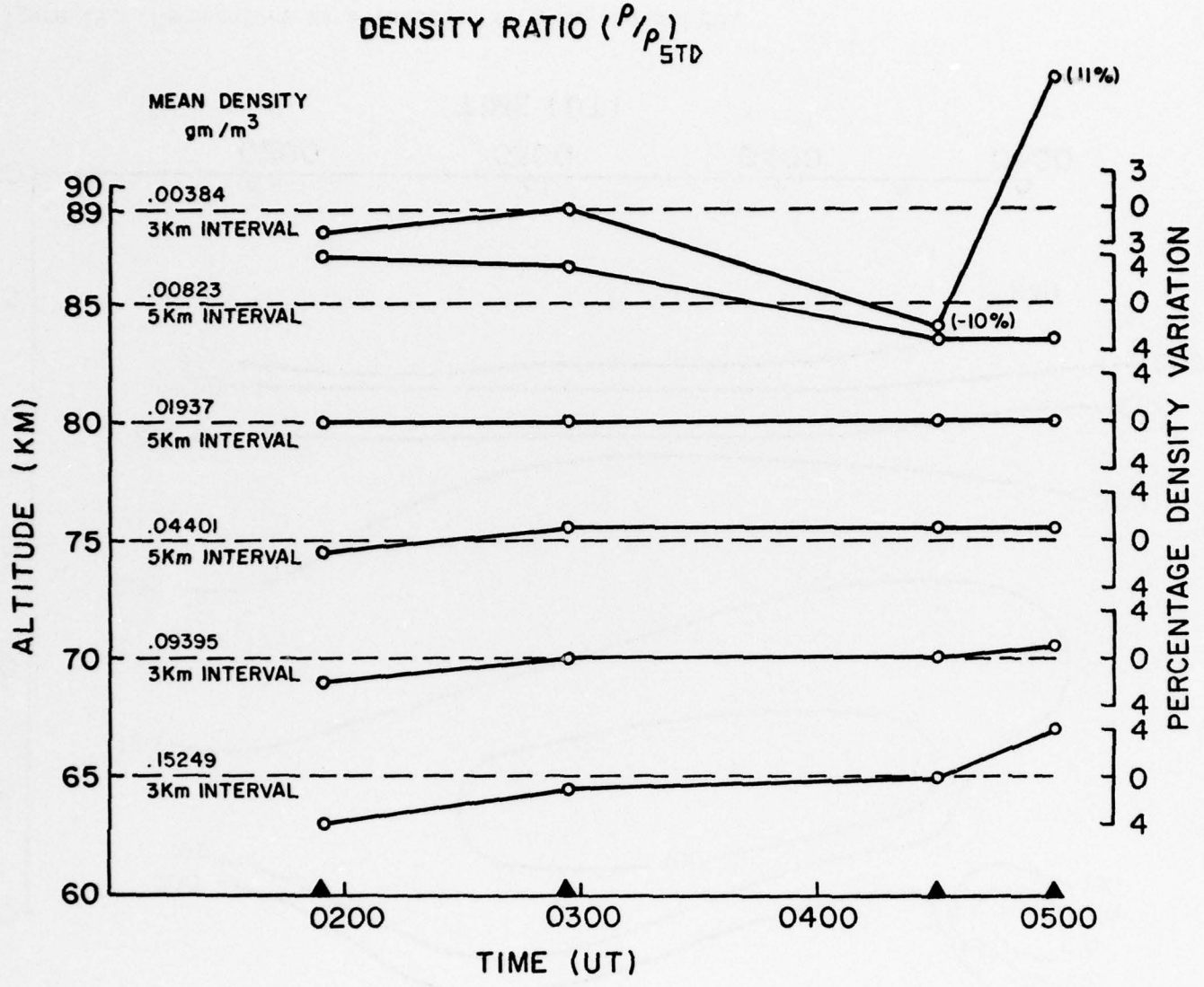

Figure 18. Density ratio as a function of time and height.

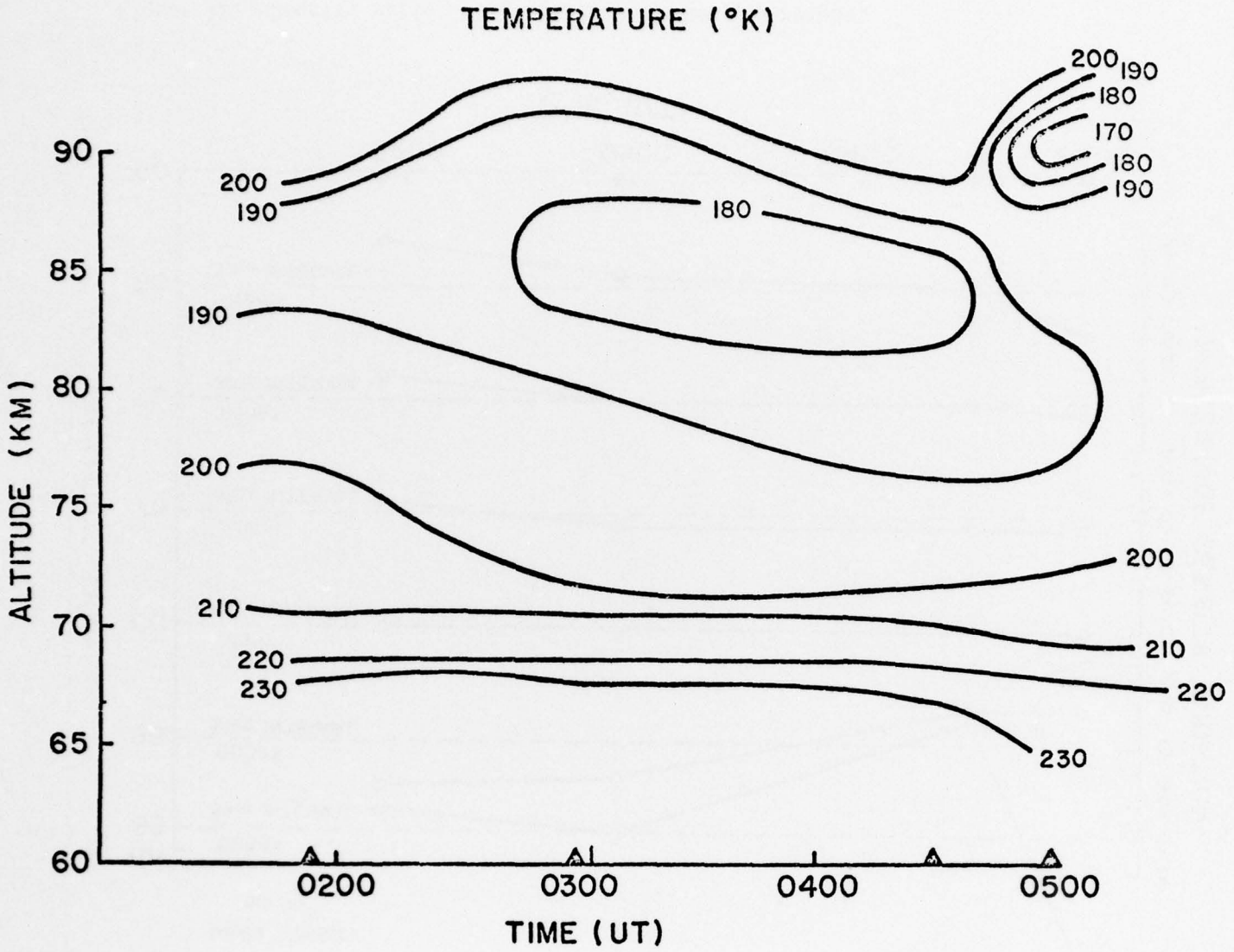

Figure 19. Temperature as a function of time and height.

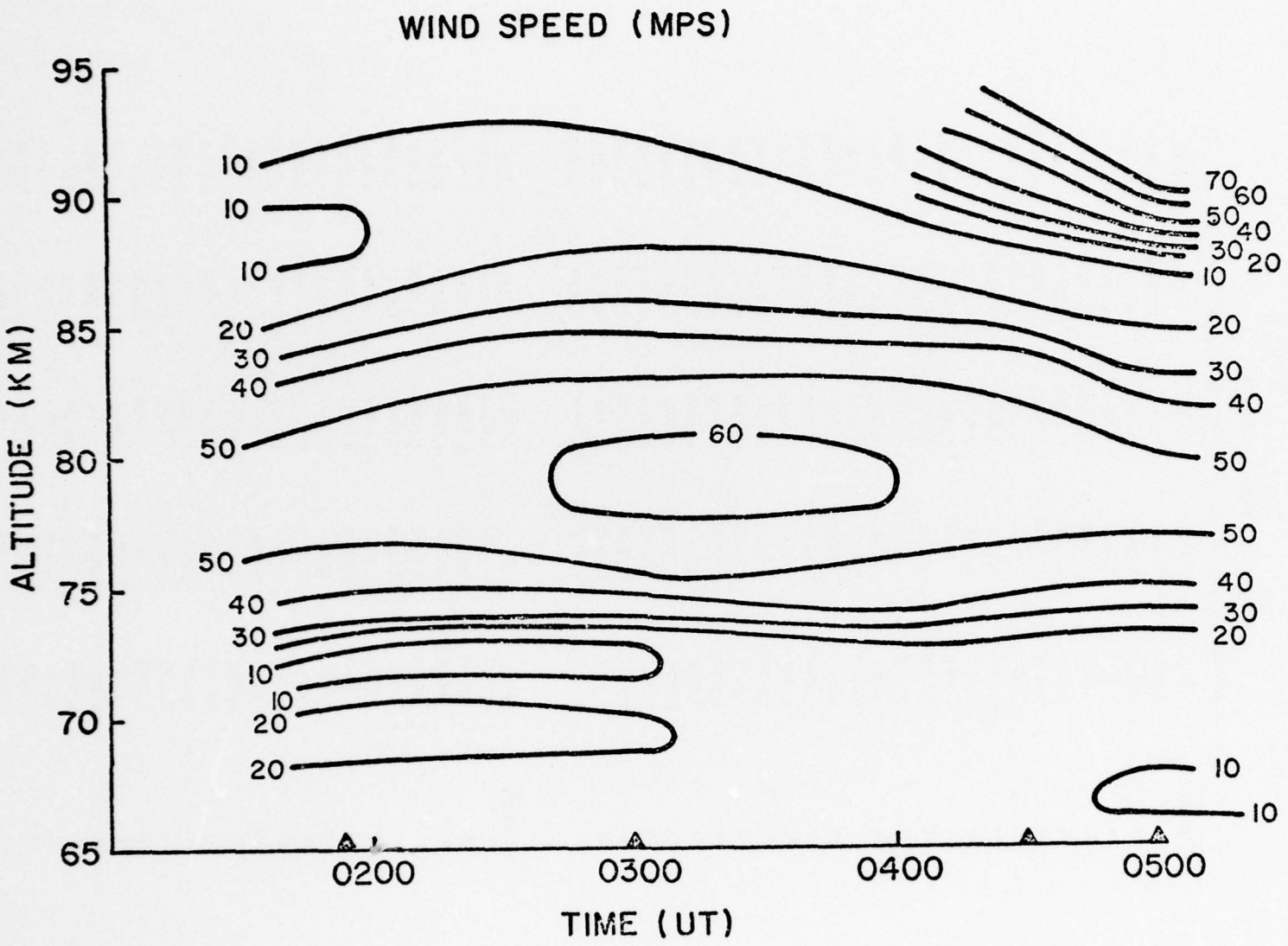

Figure 20. Wind speed as a function of time and height.

APPENDIX A. ATMOSPHERIC DENSITIES

KWAJALEIN MISSILE RANGE ROBIN SPHERE AVERAGE DENSITY VALUES (g/m^3)

Altitude(km)	2001A	2001B	2003	2005	2008
90	0.00370	0.00359	0.00297	0.00308	0.00396
89	0.00447	0.00425	0.00377	0.00379	0.00459
88	0.00525	0.00501	0.00475	0.00457	0.00516
87	0.00605	0.00588	0.00586	0.00549	0.00579
86	0.00686	0.00684	0.00709	0.00665	0.00666
85	0.00785	0.00803	0.00847	0.00809	0.00787
84	0.00918	0.00949	0.01003	0.00983	0.00950
83	0.01104	0.01120	0.01171	0.01174	0.01146
82	0.01326	0.01331	0.01352	0.01386	0.01390
81	0.01600	0.01607	0.01563	0.01614	0.01667
80	0.01938	0.01951	0.01828	0.01863	0.01984
79	0.02308	0.02349	0.02157	0.02150	0.02319
78	0.02691	0.02782	0.02544	0.02502	0.02676
77	0.03129	0.03201	0.03016	0.02929	0.03098
76	0.03565	0.03696	0.03605	0.03492	0.03540
75	0.04130	0.04257	0.04289	0.04180	0.04082
74	0.04797	0.04933	0.05086	0.04990	0.04685
73	0.05547	0.05702	0.05847	0.05885	0.05452
72	0.06387	0.06591	0.06742	0.06913	0.06410
71	0.07269	0.07587	0.07820	0.08190	0.07480
70	0.08395	0.08607	0.08948	0.09012	0.08606
69	0.09441	0.09889	0.10492	0.10578	0.10070
68	0.10997	0.11402	0.11781	0.11466	0.11682
67	0.12357	0.12535	0.13242	0.12540	0.12923
66	0.14485	0.14649	0.15335	0.14604	0.14917
65	0.16914	0.17333	0.16874	0.16817	0.16793

Altitude(km)	2009	2011	2012	2015	2016
90	0.00383	0.00298	0.00313	0.00290	0.00368
89	0.00444	0.00371	0.00380	0.00341	0.00417
88	0.00514	0.00466	0.00460	0.00411	0.00472
87	0.00598	0.00580	0.00559	0.00506	0.00537
86	0.00693	0.00706	0.00678	0.00623	0.00624
85	0.00807	0.00842	0.00824	0.00765	0.00742
84	0.00948	0.00984	0.00994	0.00945	0.00893
83	0.01114	0.01146	0.01177	0.01143	0.01074
82	0.01319	0.01353	0.01381	0.01363	0.01287
81	0.01581	0.01604	0.01615	0.01609	0.01546
80	0.01901	0.01898	0.01892	0.01889	0.01862
79	0.02262	0.02233	0.02224	0.02208	0.02214
78	0.02655	0.02614	0.02597	0.02578	0.02622
77	0.03115	0.03082	0.03078	0.03056	0.03105
76	0.03602	0.03592	0.03607	0.03609	0.03675
75	0.04178	0.04232	0.04312	0.04306	0.04311
74	0.04841	0.04927	0.05108	0.05141	0.05104
73	0.05598	0.05758	0.06016	0.06045	0.05962
72	0.06593	0.06819	0.07060	0.07092	0.06937
71	0.07863	0.08001	0.08212	0.08195	0.08178
70	0.09019	0.09041	0.09244	0.09213	0.09352
69	0.10446	0.10521	0.10758	0.10647	0.10790
68	0.12120	0.11658	0.11908	0.12039	0.12243
67	0.13430	0.12877	0.13270	0.13362	0.13749
66	0.15202	0.14665	0.15197	0.15222	0.15737
65	0.17207	0.16520	0.17022	0.17183	0.18184

APPENDIX B. TEMPERATURES

KWAJALEIN MISSILE RANGE ROBIN SPHERE AVERAGE TEMPERATURE VALUES (°K)

Altitude(km)	2001A	2001B	2003	2005	2008
90	186.0	189.0	200.5	178.3	144.5
89	184.0	190.0	187.0	175.7	155.5
88	187.5	192.0	177.5	175.7	170.0
87	193.5	194.0	173.5	176.7	182.5
86	201.5	197.0	173.5	175.3	189.5
85	207.0	199.0	175.5	174.3	190.5
84	208.0	198.0	178.5	173.7	188.0
83	203.0	199.0	184.0	175.7	186.5
82	199.5	198.0	188.0	179.3	183.5
81	195.0	194.0	195.5	184.7	183.5
80	191.5	190.0	197.5	191.0	184.5
79	191.0	188.0	198.0	196.3	188.5
78	195.0	189.0	198.5	199.3	194.0
77	198.0	193.5	197.5	201.0	199.0
76	205.0	198.5	196.0	199.0	205.0
75	208.0	203.5	195.0	196.3	208.5
74	210.0	206.5	195.0	195.0	213.0
73	212.5	209.5	201.0	196.0	213.5
72	215.5	212.0	205.0	197.3	212.5
71	220.5	215.5	207.5	201.3	213.0
70	231.5	221.0	212.5	210.7	216.0
69	227.5	223.5	212.0	210.0	215.5
68	226.0	225.0	220.5	226.3	216.5
67	232.5	237.0	227.0	238.3	227.5
66	229.0	233.0	227.5	235.3	228.5
65	227.0	227.5	238.5	235.5	234.5

Altitude(km)	2009	2011	2012	2015	2016
90	172.5	215.5	186.5	201.0	166.0
89	180.0	202.5	184.0	202.0	176.5
88	185.5	190.5	181.5	197.0	187.5
87	190.5	183.0	180.0	190.5	196.0
86	195.0	180.5	178.0	184.0	199.0
85	198.5	181.5	176.5	179.5	197.5
84	199.5	186.0	176.5	175.5	194.5
83	200.0	190.0	179.5	175.0	192.0
82	199.5	192.0	183.5	177.0	190.5
81	197.0	192.5	187.5	180.5	189.0
80	194.0	193.0	191.0	184.5	187.0
79	193.5	194.5	193.0	188.5	187.5
78	195.5	196.5	196.0	192.5	189.0
77	197.5	197.5	196.0	192.5	190.0
76	201.5	200.5	197.5	193.5	191.0
75	204.5	200.5	196.0	193.0	193.5
74	207.0	203.0	196.0	192.0	194.0
73	210.5	204.0	197.0	194.0	197.0
72	209.5	203.5	199.0	196.0	200.0
71	206.0	204.0	202.0	200.5	200.0
70	211.0	212.0	210.5	209.5	206.5
69	212.5	212.5	211.5	212.5	210.0
68	214.5	223.5	223.0	219.5	216.0
67	225.0	234.0	232.0	229.0	224.0
66	230.0	237.5	233.5	232.5	227.0
65	234.5	241.5	240.5	237.5	227.0

APPENDIX C. WIND SPEED AND DIRECTION

KWAJALEIN MISSILE RANGE ROBIN SPHERE AVERAGE WIND VALUES

	2001A		2001B		2003		2005		2008	
Altitude(km)	Speed	Direction	Speed	Direction	Speed	Direction	Speed	Direction	Speed	Direction
90	41	222	21	214	31	175	27	151	70	22
89	39	207	33	192	37	291	21	138	65	31
88	39	195	43	182	50	279	21	285	60	42
87	39	185	50	178	58	271	31	285	54	51
86	37	180	52	175	61	214	40	282	48	64
85	34	181	49	175	62	259	45	279	44	79
84	31	183	43	176	61	253	47	275	43	96
83	27	185	35	178	58	249	47	271	44	112
82	22	189	28	181	52	247	46	266	46	126
81	17	198	20	189	46	239	44	260	47	138
80	12	207	13	206	38	233	40	252	49	147
79	8	226	9	242	30	226	35	241	50	152
78	7	271	12	277	22	214	30	227	50	155
77	9	305	17	275	14	192	26	209	48	154
76	14	315	21	285	10	145	23	187	45	152
75	20	309	25	288	13	95	22	165	41	145
74	24	318	28	288	20	73	20	144	36	135
73	28	315	30	288	25	60	16	120	33	121
72	32	312	32	288	27	46	12	79	30	105
71	33	312	32	290	28	30	15	27	27	89
70	29	316	29	296	28	11	23	354	21	74
69	23	337	23	213	27	347	30	338	14	54
68	22	13	19	352	27	320	31	324	7	179
67	27	40	24	30	27	302	24	316	11	292
66	27	48	29	44	23	303	12	322	21	285
65	21	53	28	45	14	333	6	40	29	289

	2009		2011		2012		2015		2016	
Altitude(km)	Speed	Direction	Speed	Direction	Speed	Direction	Speed	Direction	Speed	Direction
90	61	39	14	76	14	178	48	183	72	15
89	60	40	10	108	17	165	32	349	53	9
88	57	46	10	133	18	154	18	326	34	184
87	50	53	12	133	21	136	9	271	16	181
86	44	64	18	123	26	118	12	187	7	169
85	40	77	26	115	33	107	23	156	13	151
84	36	91	34	108	42	99	32	140	22	142
83	35	106	42	103	49	94	42	130	29	132
82	36	119	48	100	55	91	49	122	37	122
81	38	130	52	96	59	88	54	115	43	114
80	41	137	55	94	62	87	58	108	48	107
79	43	141	58	93	62	86	59	101	51	100
78	44	143	58	93	61	84	58	95	52	94
77	43	143	55	93	57	84	55	88	51	88
76	40	139	50	93	51	83	49	81	47	82
75	36	133	42	92	42	81	42	69	41	77
74	32	123	31	93	31	79	32	56	31	70
73	28	108	17	93	18	72	24	35	20	54
72	26	88	4	67	7	28	18	359	11	9
71	24	69	14	292	11	297	18	324	13	309
70	20	51	24	292	20	279	18	300	16	284
69	13	33	29	297	22	268	13	268	14	262
68	6	344	25	299	18	256	11	222	11	235
67	9	262	18	304	15	253	12	207	9	241
66	15	263	14	315	15	273	12	254	10	290
65	22	274	12	327	17	288	16	286	18	311